Goals and Status of neutron skin measurements

PREX, PREX-II, CREX and MREX

MREX

Juliette Mammei

University of Manitoba

Jefferson Lab

NSERC CRSNG

JSA

JG|U Johannes Gutenberg Universität Mainz

Connecting heaven and earth

Crab Nebula (X-ray, infrared, radio, visible)

If PREX II (and other earth-based experiments) confirm that R_{skin} is large, and astrophysical observations, including new LIGO-Virgo evidence, continue to suggest that NS-radius is small, this may be evidence of a softening of the EOS at high densities

$\Rightarrow$ phase transition

Gravitational

electric dipole polarizability
heavy ion collisions
spectroscopy (diff. isotopes)
coherent neutrino scattering

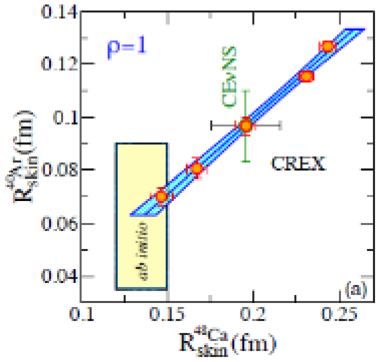

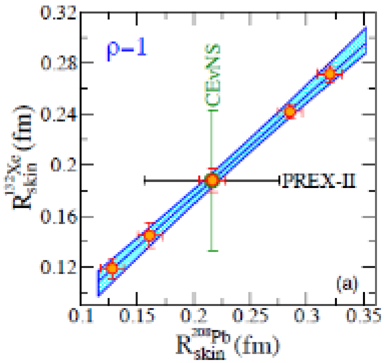

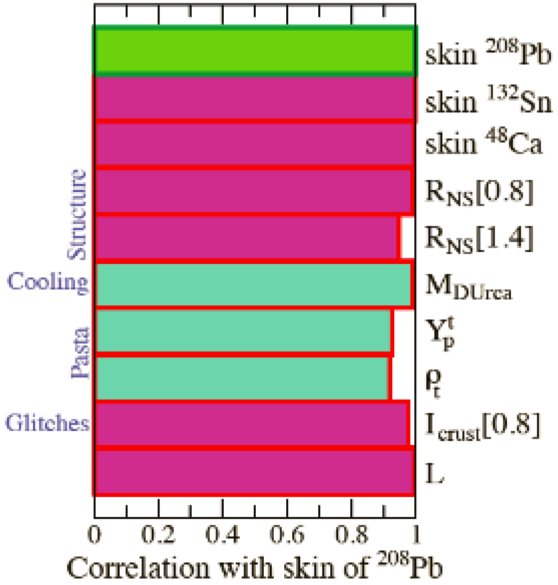

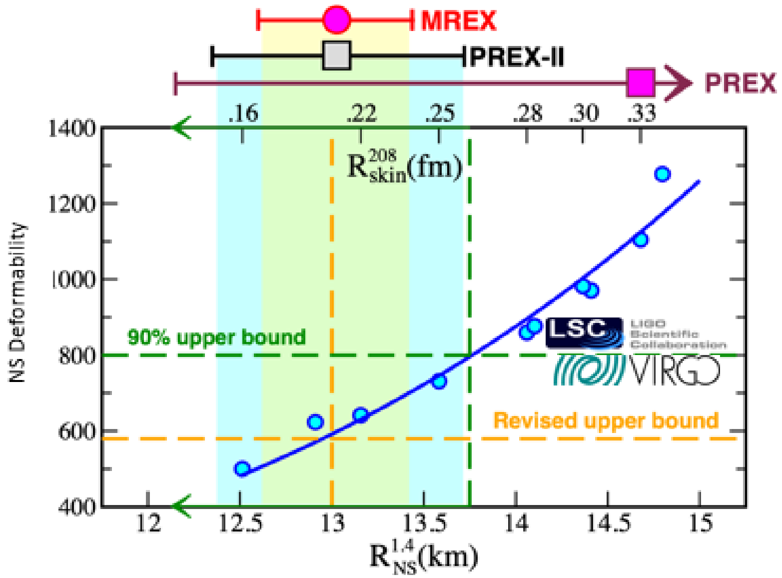

Parity-violating electron scattering facilities JLAB and Mainz

vectorstock.com/29644663

Neutron skin with PVES

$$A_{PV} = \frac{\sigma_+ - \sigma_-}{\sigma_+ + \sigma_-} \approx$$

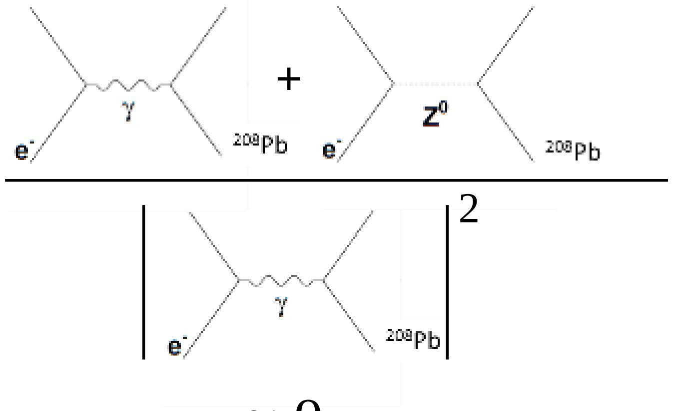

$$= \frac{G_F Q^2}{2\pi\alpha\sqrt{2}} \left[\overbrace{1 - 4\sin^2\theta_W}^{\approx 0} - \frac{F_n(Q^2)}{F_p(Q^2)} \right]$$

The Fourier transform of the weak "form factor" $F_W(Q^2)$ gives the weak charge density as a function of radius, just as the FT of the charge form factor gives the charge density

$$Q^p_{weak} = 1 - 4\sin^2\theta_W \approx 0$$

$$Q^n_{weak} = -1$$

neutron density

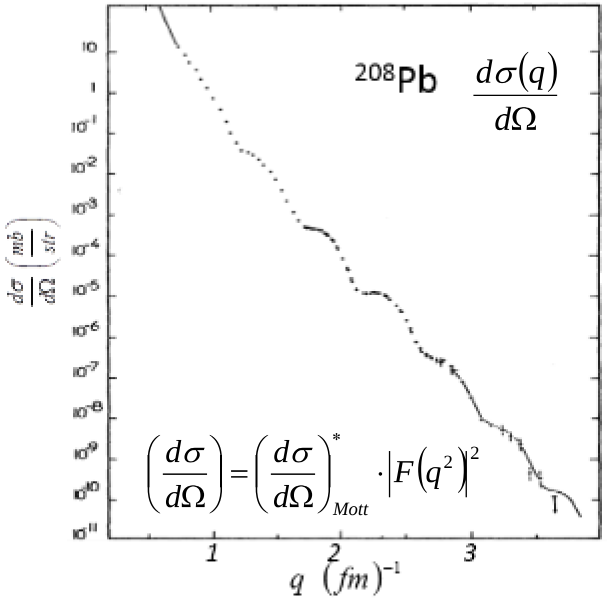

$$F_n(Q^2) = \frac{1}{4\pi} \int d^3r \ j_0(qr) \ \rho_n(r)$$

Measurement of $F_n(Q^2)$ at a single Q^2 translates to a measurement of R_n via mean-field nuclear models

At low Q^2 there is a tight correlation between R_n and $F_n(Q^2)$

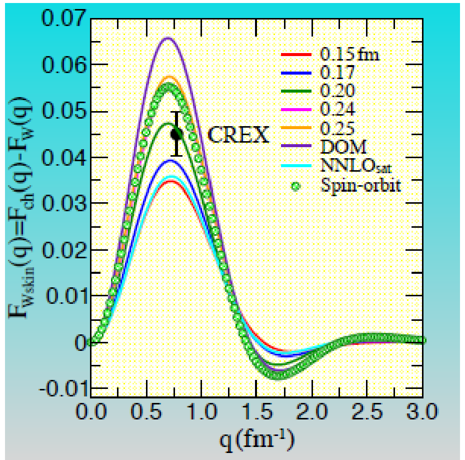

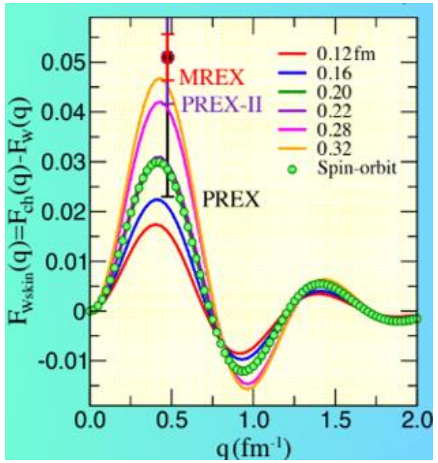

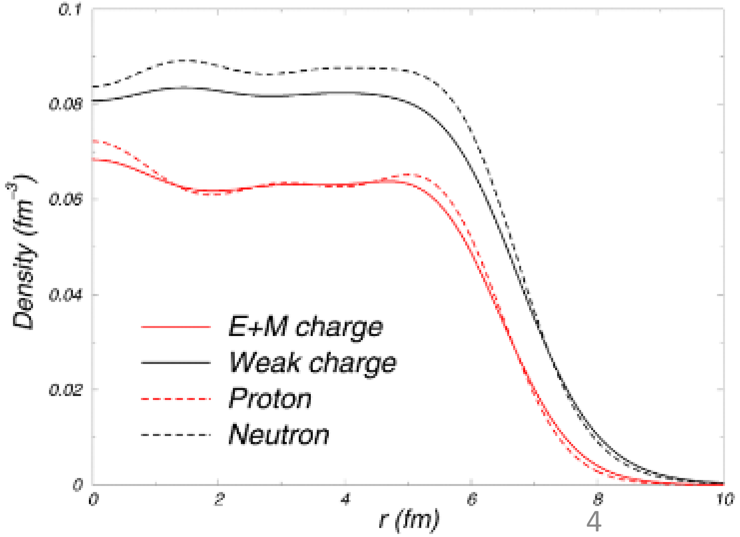

Why lead and calcium?

- First excited state far from elastic peak
- Target that won't melt
- Neutron excess
- Doubly-magic
- Stable

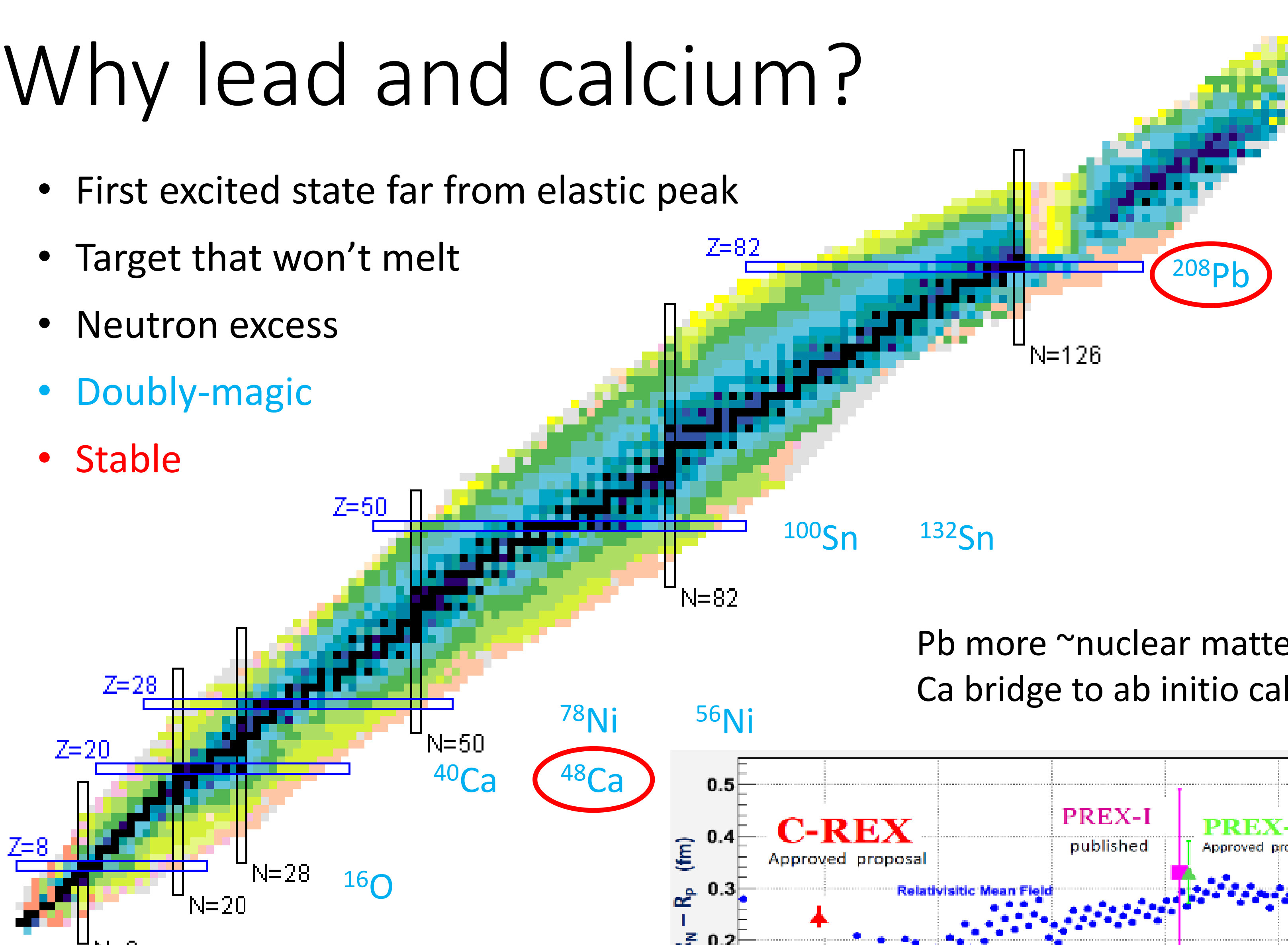

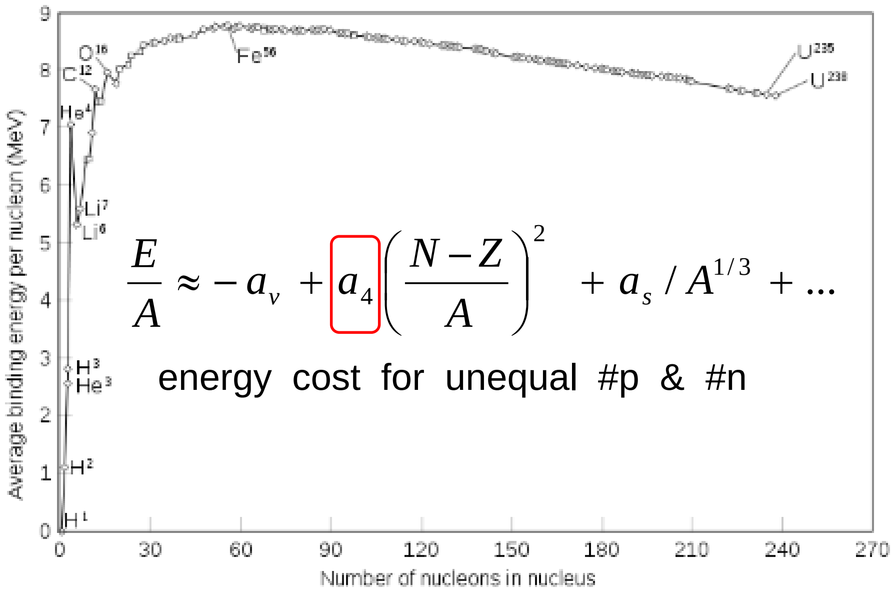

$$\frac{E}{A} \approx -a_v + \boxed{a_4}\left(\frac{N-Z}{A}\right)^2 + a_s / A^{1/3} + \ldots$$

energy cost for unequal #p & #n

Pb more ~nuclear matter;
Ca bridge to ab initio calcs.

Test models over a large range of A

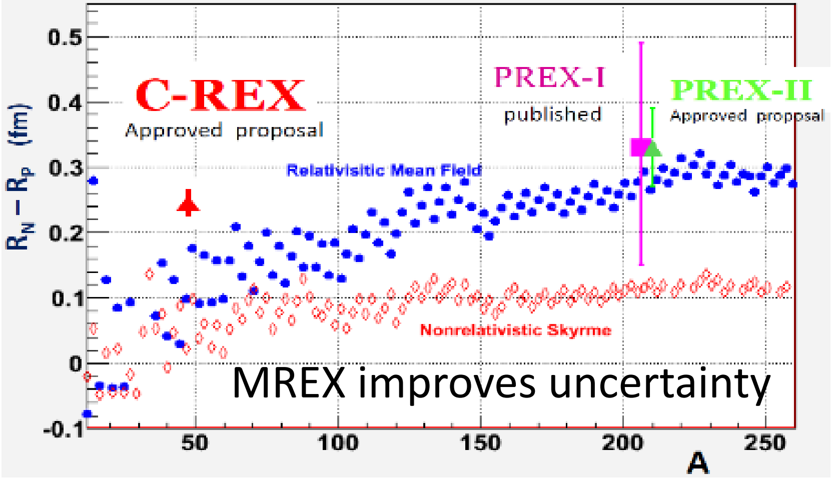

MREX improves uncertainty

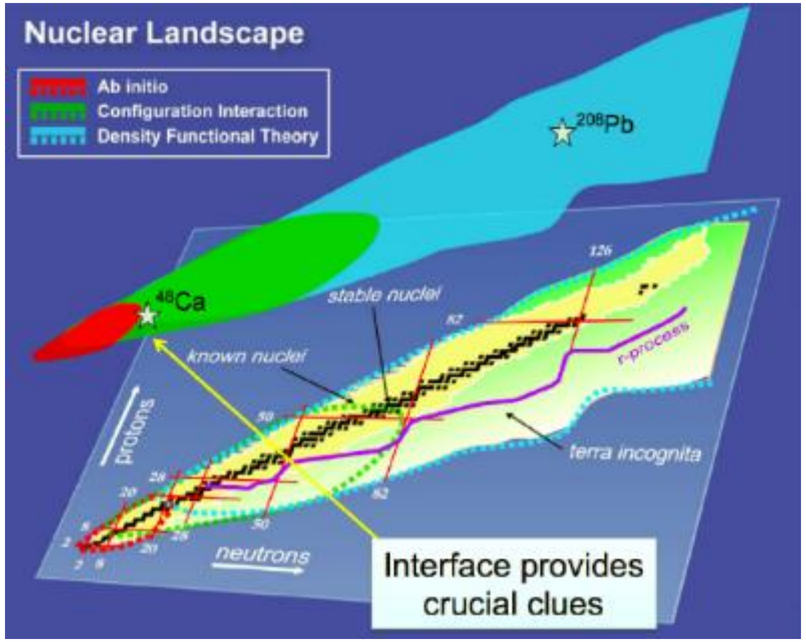

“Steps” to measure A_{PV} with PVES

- unpolarized target
- high current
- highly polarized beam

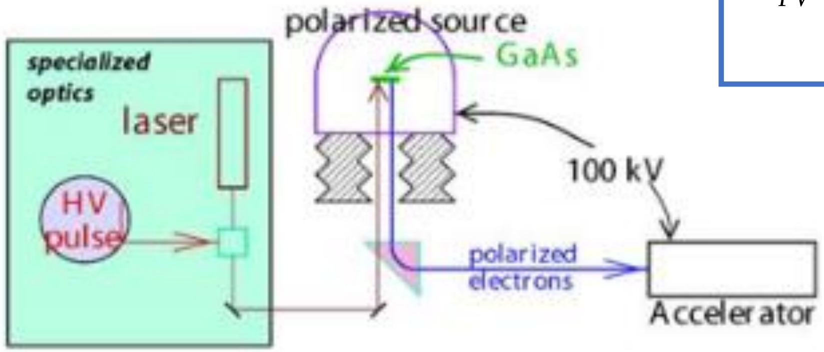

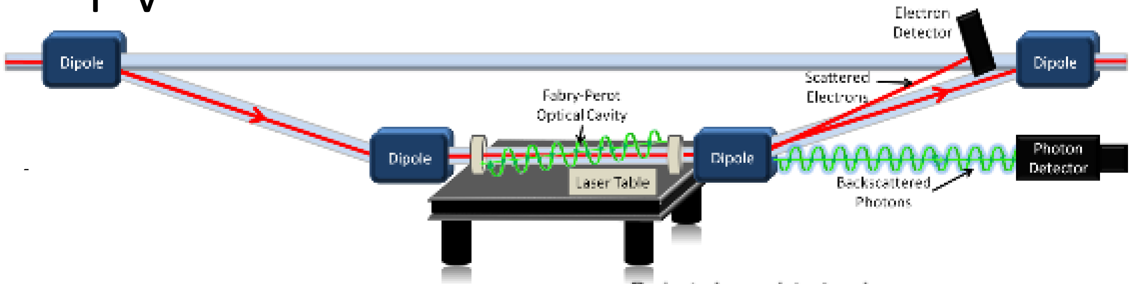

A_{PV}

$$A_{sig} = \frac{A_{corr} - A_{back}\ f_{back}}{f_{sig}}$$

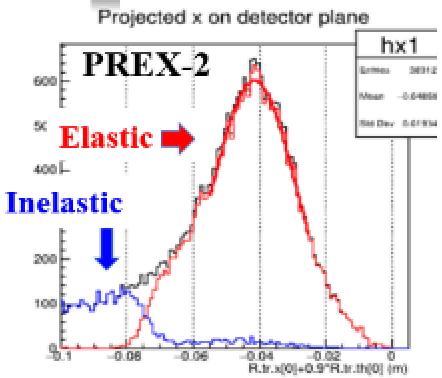

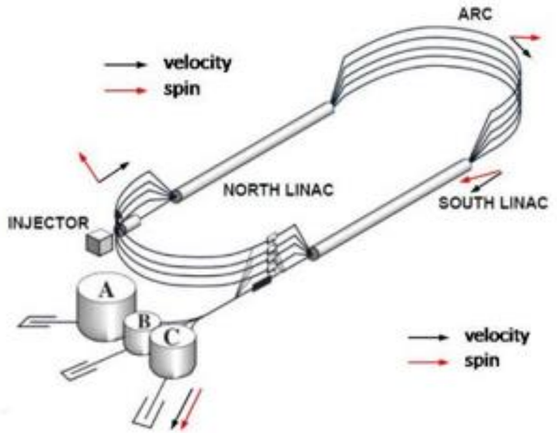

- polarimetry
- elastic electrons from target
  (resolution of the spectrometer)
- beam property monitoring
- active feedback to minimize helicity correlations
- rapid helicity reversal
- slow helicity reversal as a cross check

$$A_{corr} = A_{meas} - \sum_{i=1}^{N} \frac{1}{2Y}\left(\frac{\partial Y}{\partial P_i}\right)\Delta P_i$$

where $\Delta P_i = P_+ - P_-$

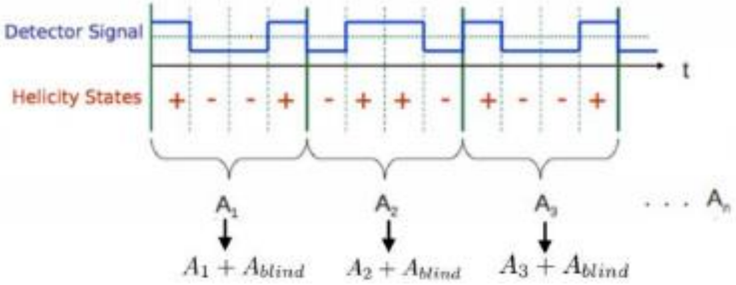

A_{meas}

PREx Results

$$A_{PV} = 0.656\ ppm \pm\ 0.060(stat) \pm 0.013(syst)$$

$$R_n - R_p = 0.33^{+16}_{-18}\ fm$$

Systematic Error	Absolute (ppm)	Relative (%)
Polarization (1)	0.0071	1.1
Beam Asymmetries (2)	0.0072	1.1
Detector Linearity	0.0071	1.1
Beam current normalization	0.0010	0.2
Rescattering	0.0001	0
Transverse Polarization	0.0012	0.2
Q^2 (1)	0.0028	0.4
Target Thickness	0.0005	0.1
^{12}C Asymmetry (2)	0.0025	0.4
Inelastic States	0	0
TOTAL	0.0130	2.0

(1) Normalization Correction applied
(2) Nonzero correction (the rest assumed zero)

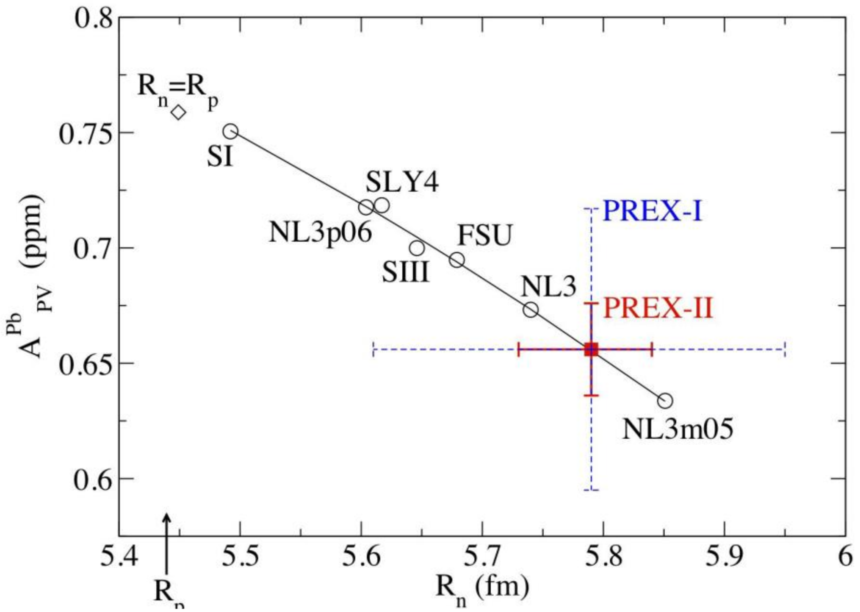

PREX-1 suffered from complications due to irradiation of various components which limited the amount of data we could collect

→ Statistics limited (9%)

→ Systematic error goal achieved !

The JLAB “Rex’s”

~1 (2.2) GeV electron beam, 70 (150) μA

high polarization, ~89%

helicity reversal at 120 Hz

PREX (CREX) Parameters

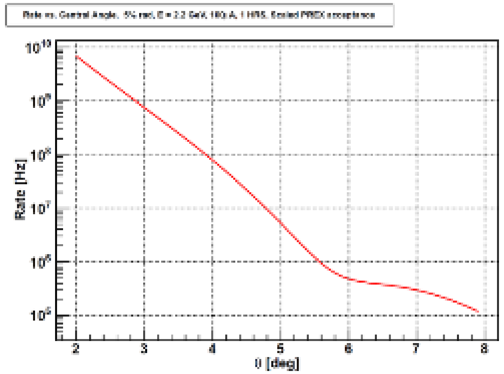

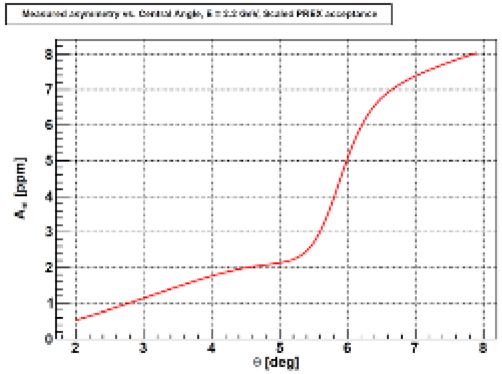

$$A_{meas} = \frac{Y_+ - Y_-}{Y_+ + Y_-}$$

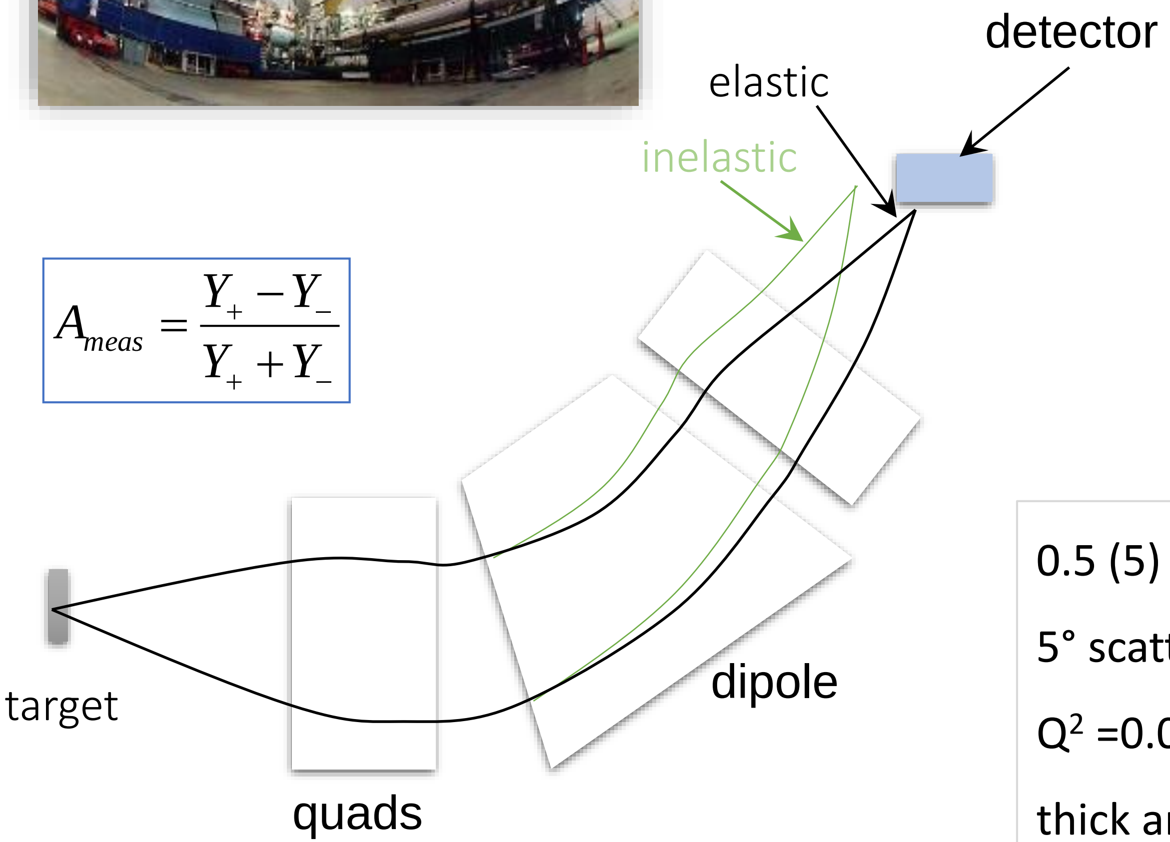

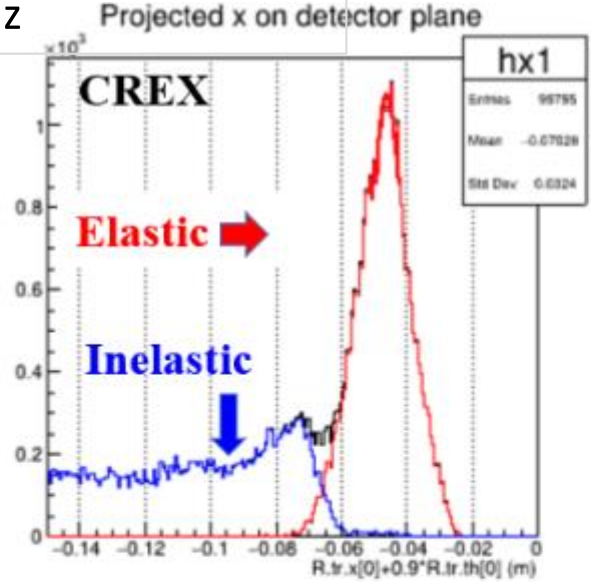

0.5 (5) mm thick Pb (Ca) target

5° scattered electrons

Q^2 =0.006 (0.03) GeV^2/c^2

thick and thin quartz detectors

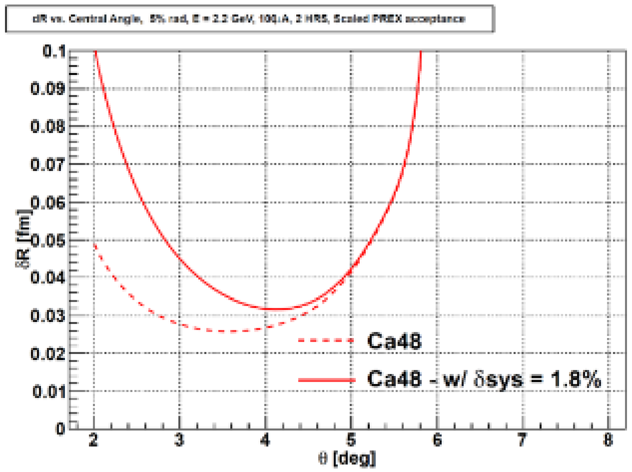

Polarized Electron Source

"Figure of Merit" $\propto I P_e^2$

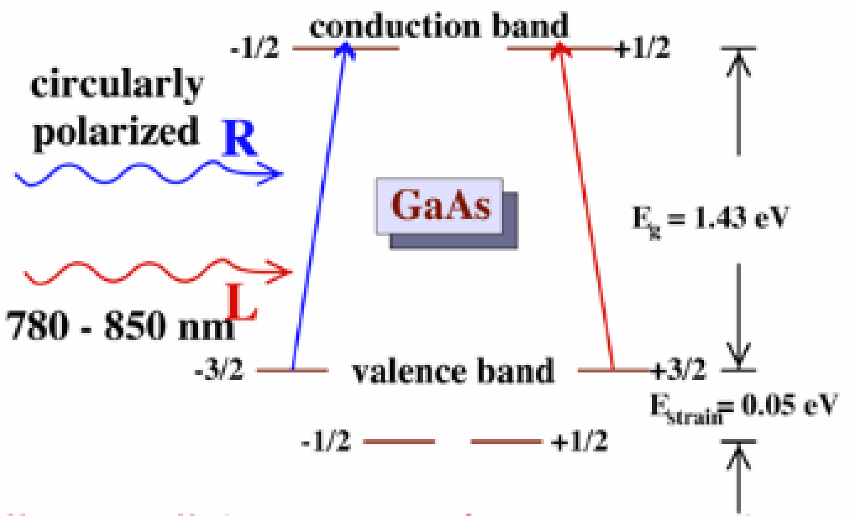

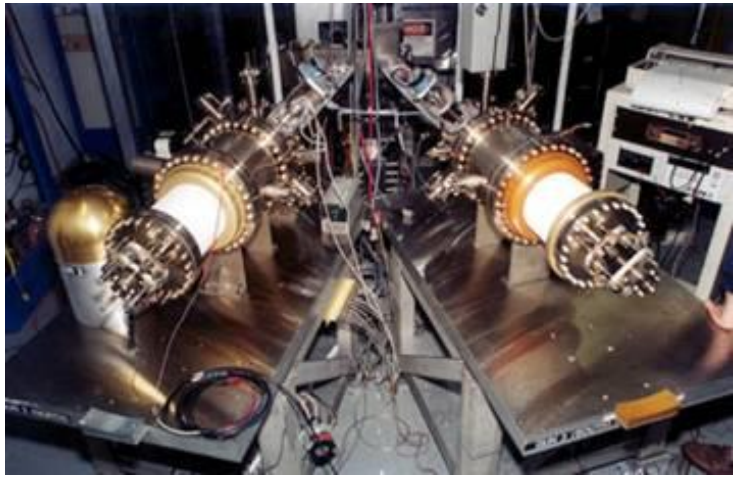

"Bulk" GaAs - typical P_e ~ 37%
(theoretical maximum - 50%)

"Strained" GaAs typical P_e ~ 80%
(theoretical maximum - 100%)

Circularly polarized laser incident on strained GaAs photocathode

Opposite helicity electrons produced by varying the voltage on a piezoelectric crystal – "Pockels cell" in order to change helicity of polarized laser light

During operation can develop a QE "hole"

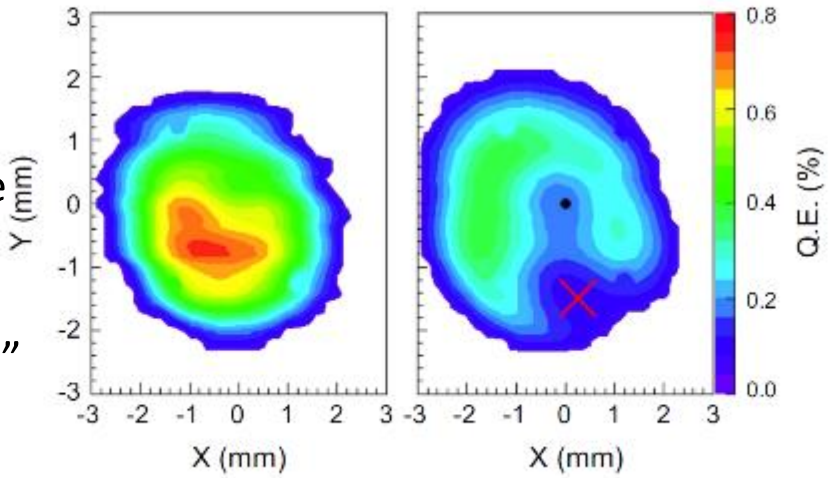

Ideally, changing the helicity of the laser would not change its position on the photocathode; in practice this is unavoidable

Much effort goes into reducing the this effect!

Helicity reversals

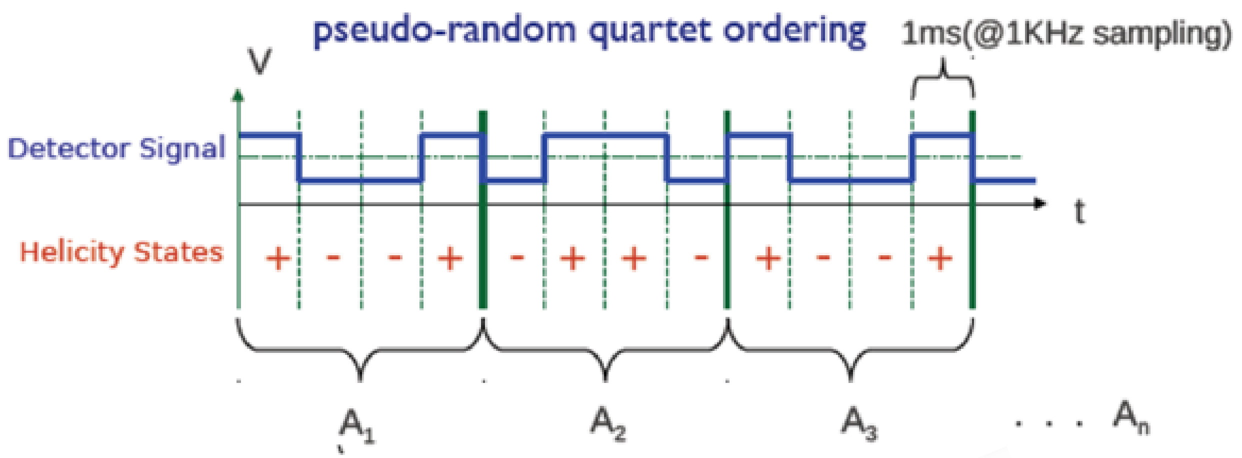

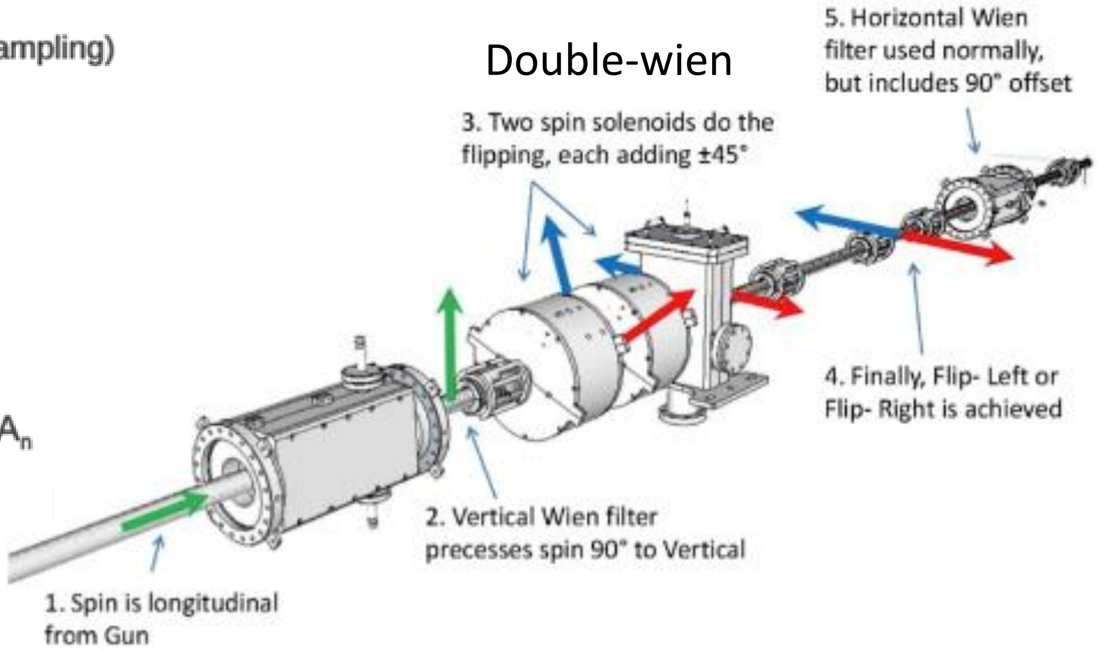

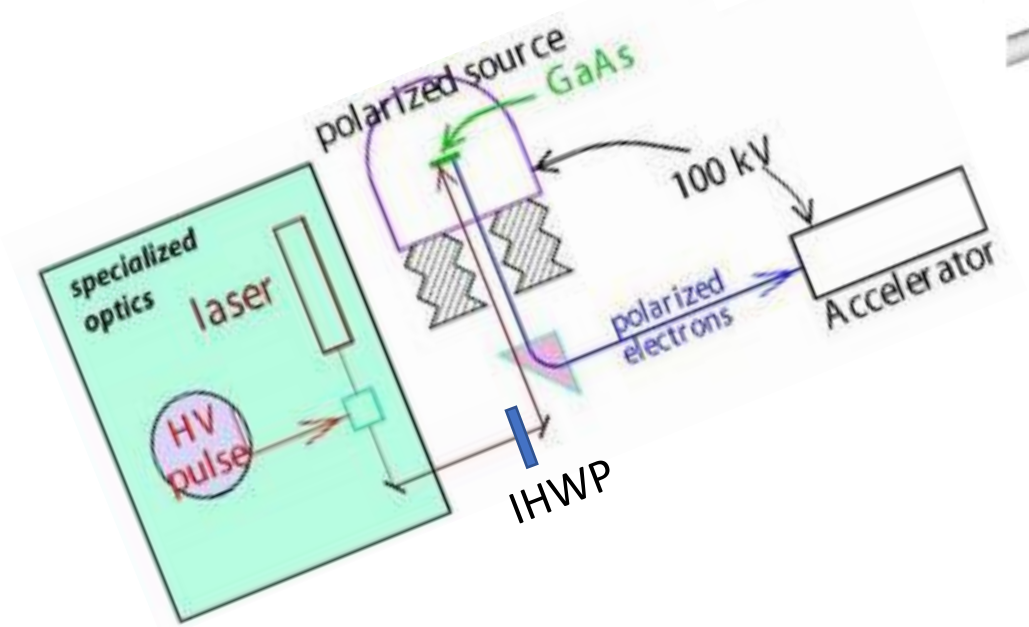

- Rapid, random helicity reversal
- Electrical isolation from the rest of the lab
- Feedback on Intensity Asymmetry
- Slow helicity reversals as a cross check
  - Insertable half-wave plate (laser)
  - Wien system (electrons)

Geometrical symmetry and 2PE

$$A_\perp^m = \frac{\sigma_\uparrow - \sigma_\downarrow}{\sigma_\uparrow + \sigma_\downarrow} = A_n \vec{p}_e \cdot \hat{n}$$

$$\hat{n} = \frac{\vec{k} \times \vec{k'}}{\left|\vec{k} \times \vec{k'}\right|}$$

- *Parity-conserving* asymmetry from interference of 2PE
- Opposite signs (same magnitude) in left- and right-HRS
- During normal running – suppressed greatly
  - Small, *horizontal* ($\vec{p}_e \cdot \hat{n} \sim 0$) component, P_T
  - Highly symmetric apparatus (A_S small)
  - Measure to determine A_n and bound uncertainty
- To measure A_n
  - Incident beam is vertically polarized
  - Change sign of vertical polarization
  - Measure fractional rate difference

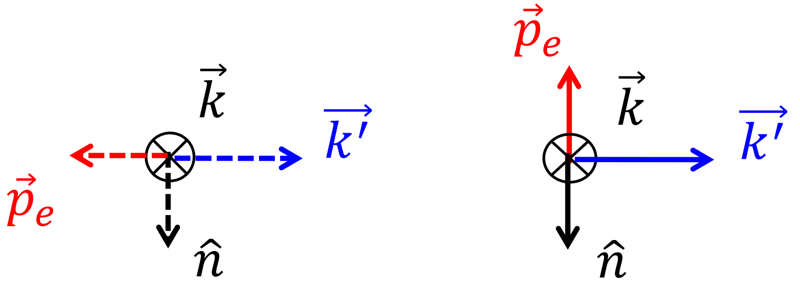

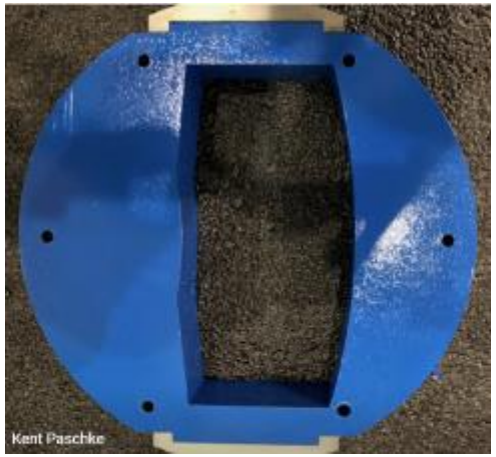

false asymmetry

transverse component

$$K_T = A_n \frac{P_T}{P} A_S$$

BNSSA

overall pol.

apparatus asymmetry

https://arxiv.org/pdf/0801.4575.pdf

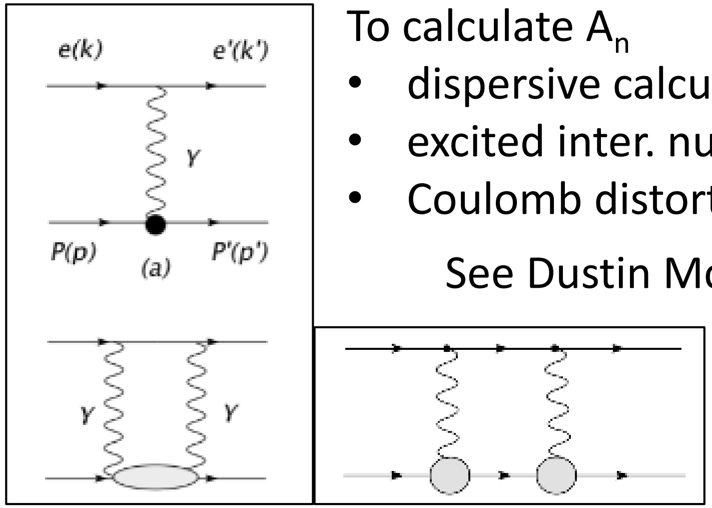

To calculate A_n
- dispersive calculations
- excited inter. nuclear states
- Coulomb distortions not included

See Dustin McNulty's talk (next)

Precision Polarimetry

Require measurement of the beam polarization to ~1%

Møller Polarimeter

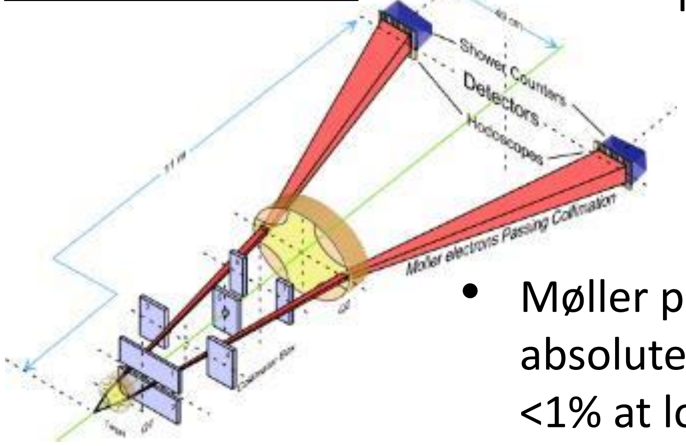

Strategy: use 2 independent polarimeters

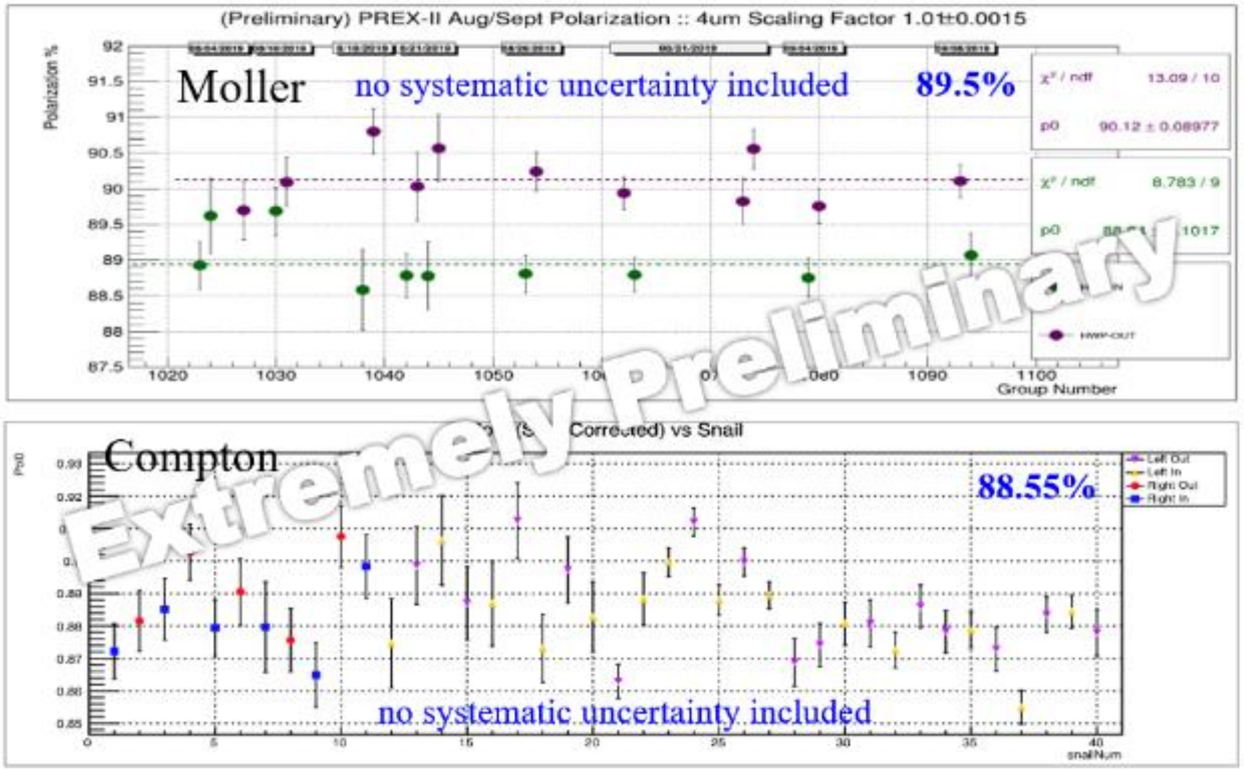

- Møller polarimeter measures absolute beam polarization to <1% at low beam currents
- Known analyzing power provided by polarized Iron foil in high magnetic field

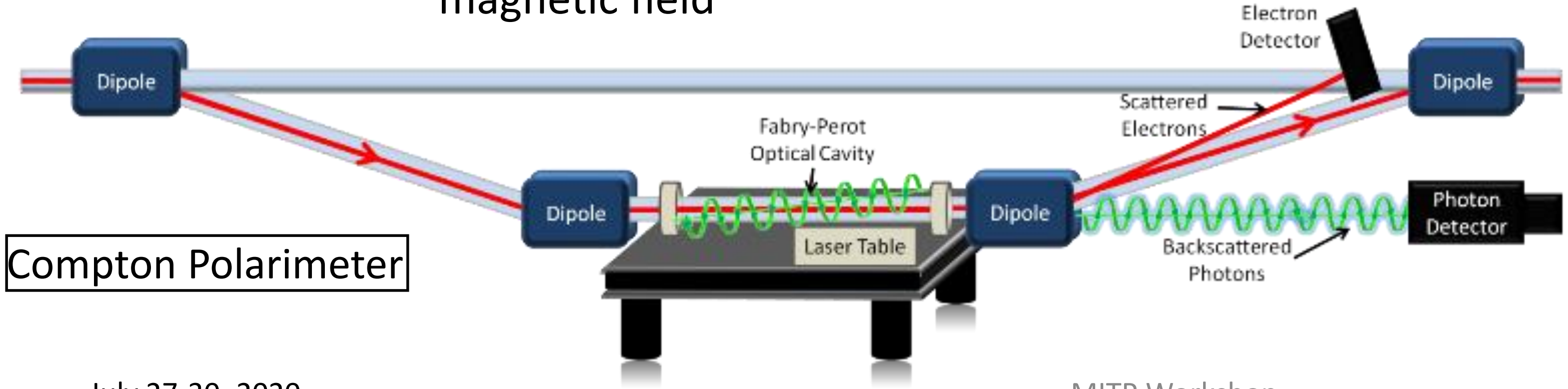

Compton Polarimeter

- Use Compton polarimeter to provide continuous, non-destructive measurement of beam polarization
- Known analyzing power provided by circularly-polarized laser beam

Linear regression and dithering - slopes

$$A_{meas} = \frac{Y^+_{meas} - Y^-_{meas}}{Y^+_{meas} + Y^-_{meas}}$$

This is the measured asymmetry

$$Y^\pm_{meas} = Y^\pm_{pv} + Y^\pm_{hc}$$

The measured yield has a part that is parity-violating and helicity-correlated yields

$$A_{meas} = \frac{Y^+_{pv} - Y^-_{pv} + \sum_m C_m \left(P^+_m - P^-_m\right)}{Y^+_{pv} + Y^-_{pv} + \sum_m C_m \left(P^+_m + P^-_m\right)}$$

$$Y^\pm_{hc} = \sum_m \frac{\partial Y_{hc}}{\partial P_m} P^\pm_m \qquad \frac{\partial Y}{\partial P_m} \equiv C_m$$

Correlation slopes, detector responses

Beam parameters

- Charge
- Energy
- horizontal/vertical position
- angles in horizontal/vertical
- size

Strategies

- measure (monitors)
- minimize (active feedback)
- correct (need detector sensitivity)
    - regress normal beam motion
    - perform dithering

Beam quality – measured and controlled

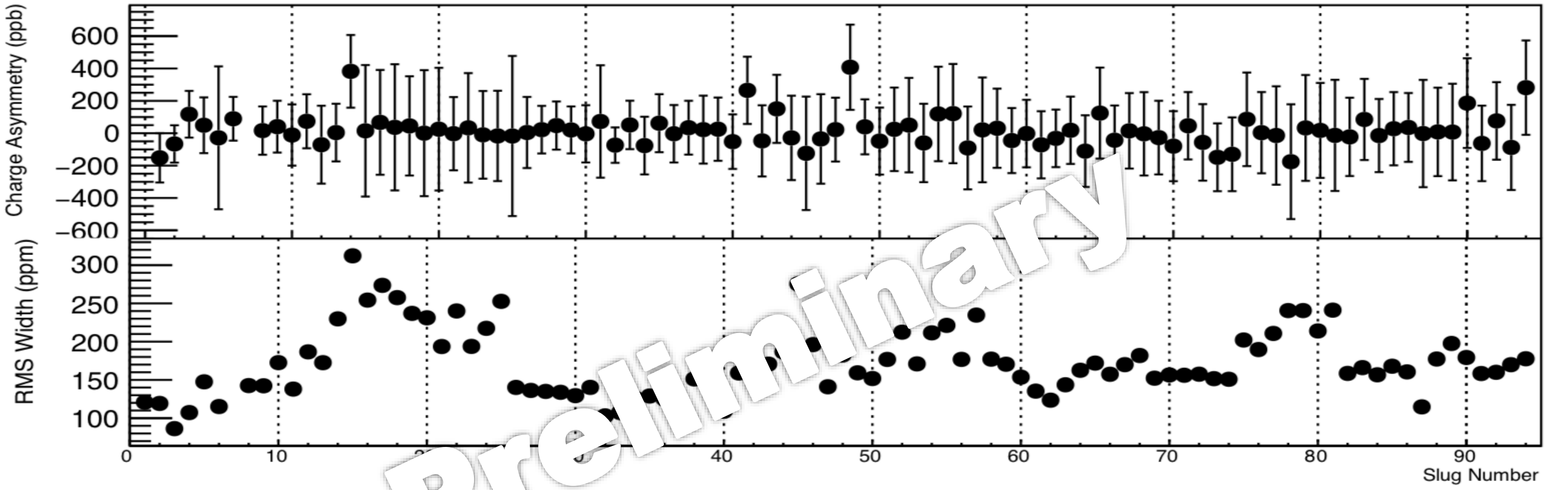

Charge asymmetries:
weighted average A_Q ~ 25 ppb

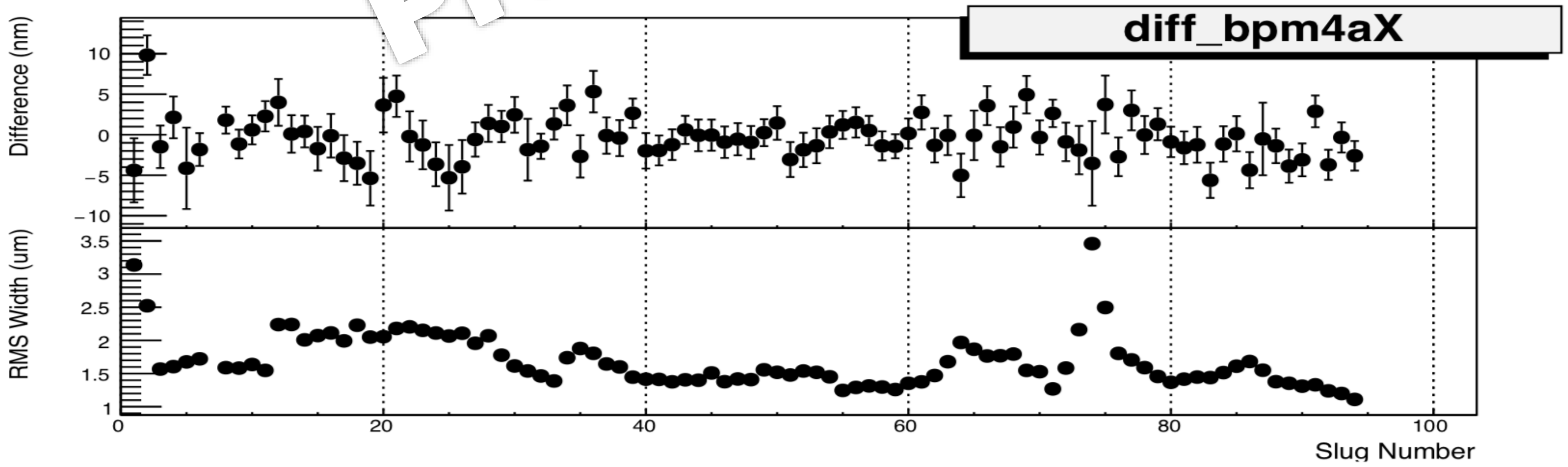

Position differences:
2 ± 2 nm

Energy asymmetry: 1 ± 0.6 ppb
Angle differences: 0.2 ± 0.4 nrad

Dithering correction effect on RMS (one slug only)

- Detector yields vary as a function of beam positions

$$A_{corr} = A_{meas} - \sum_{i=1}^{N} \frac{1}{2Y}\left(\frac{\partial Y}{\partial P_i}\right)\Delta P_i$$

where $\Delta P_i = P_+ - P_-$

- Determine slopes from dithering and linear regression
- Compare RMS of detector average (left) and difference (right)
  - before correction (top)
  - after correction (bottom)

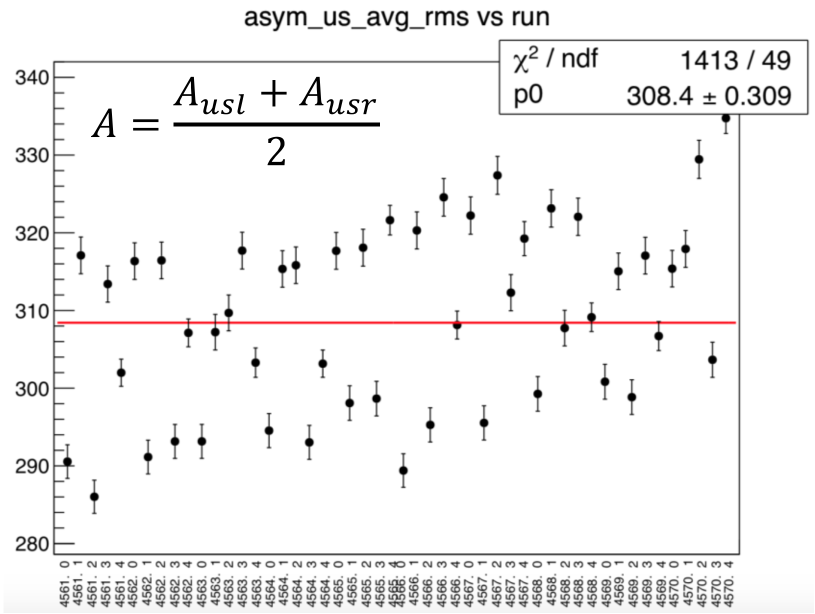

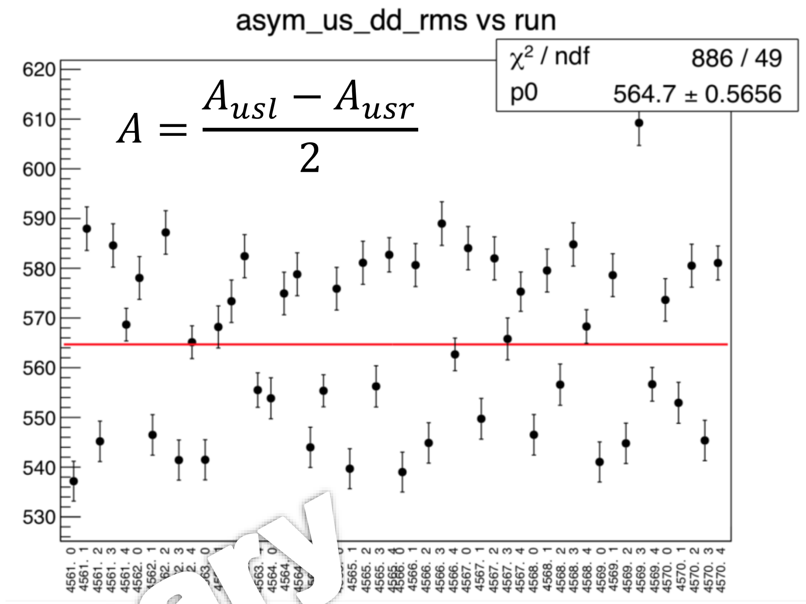

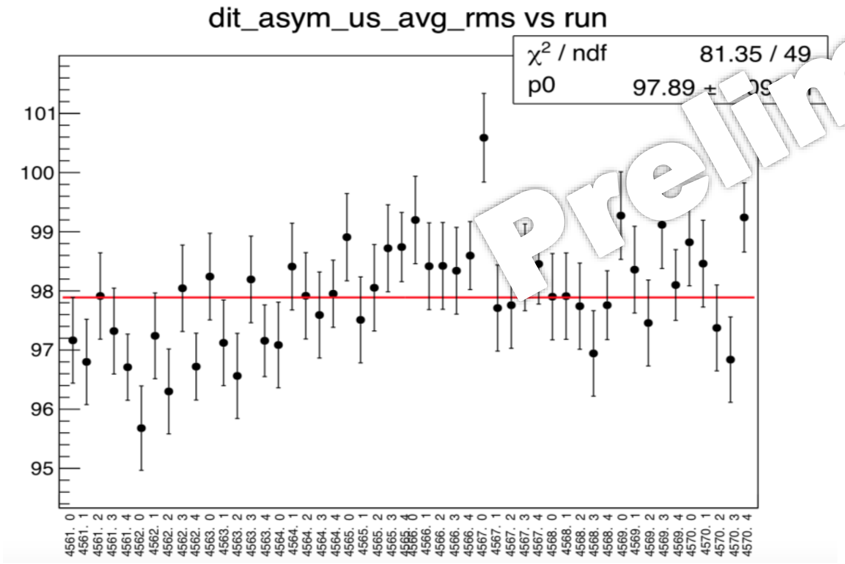

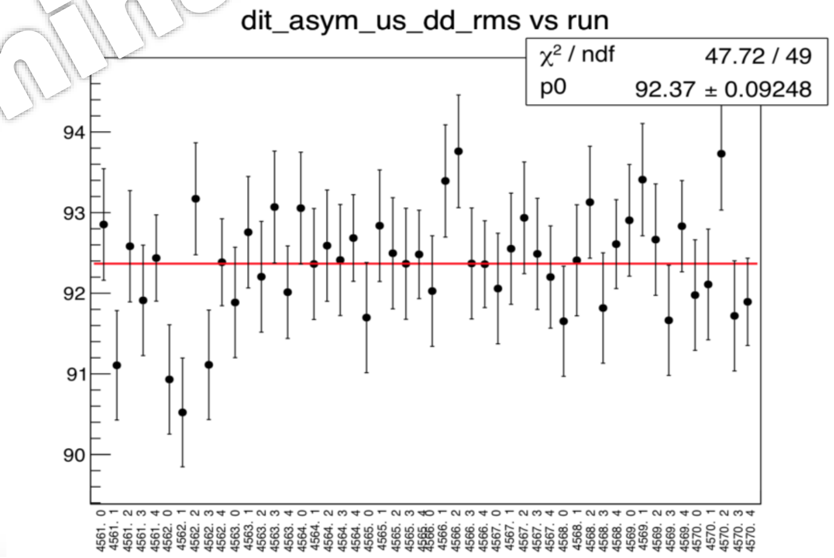

Septum magnet

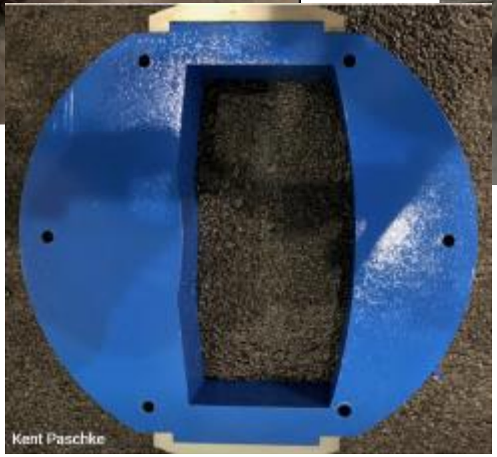

Septum magnet needed to reach the low angles

Vacuum vessel to transport scattered electrons in vacuum to detector hut

Precision collimators to define the acceptance

Extensive studies to show we could use the same config. For both PREX-2 and CREX

Integrating quartz detectors

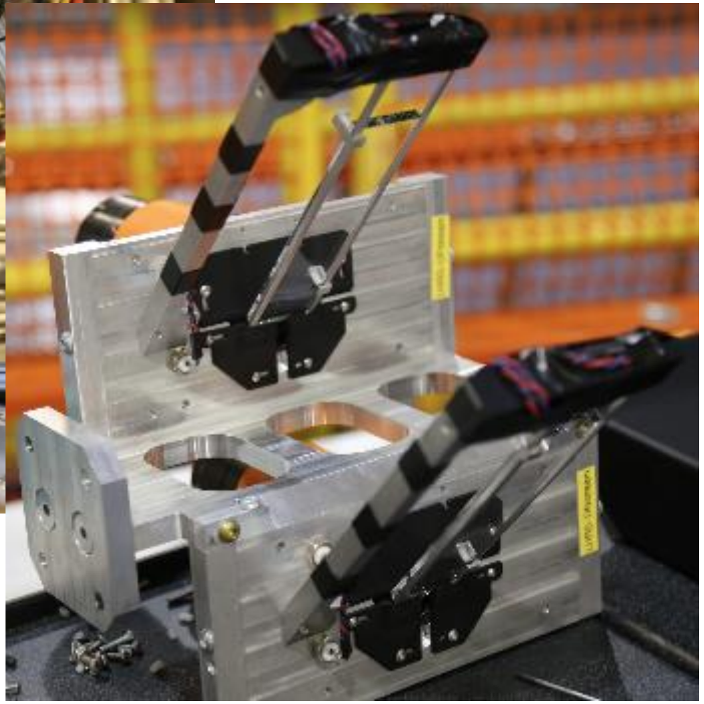

Integrating detectors (reduce deadtime effects)

Thick and thin quartz bars (different systematics)

Targets

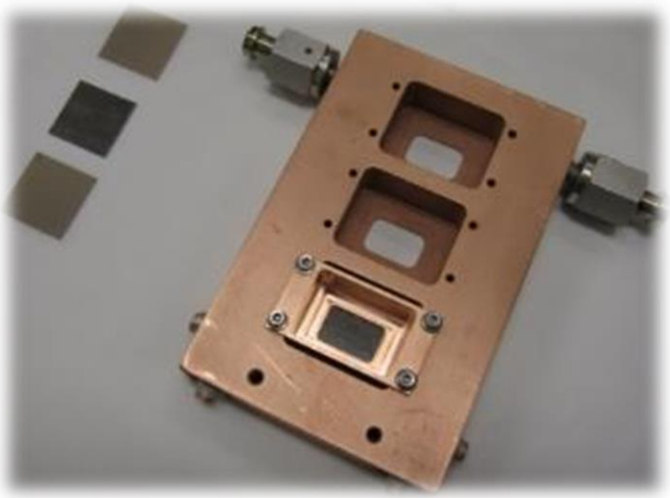

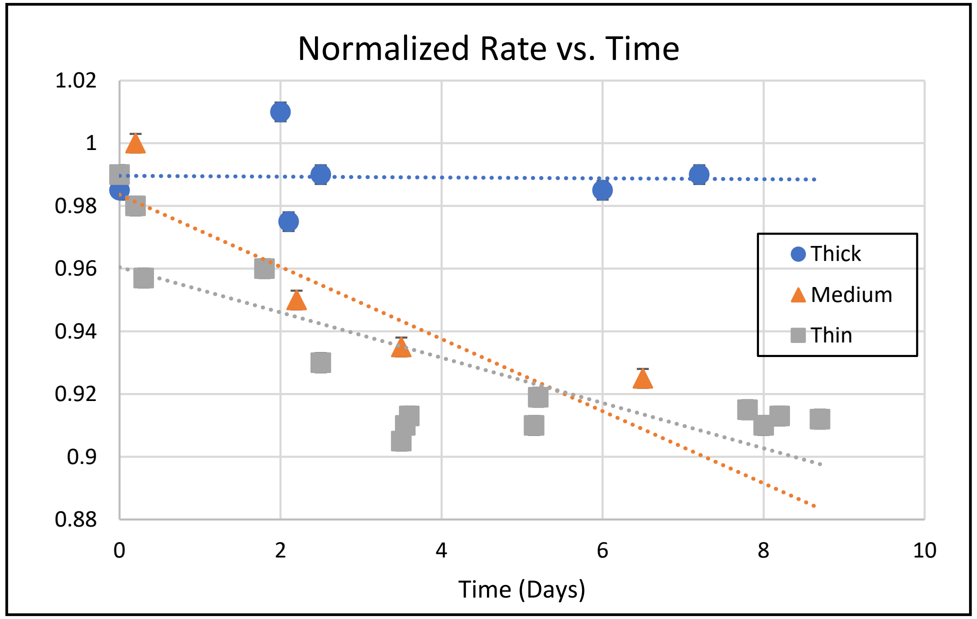

Natural Ca used in testing oxidation

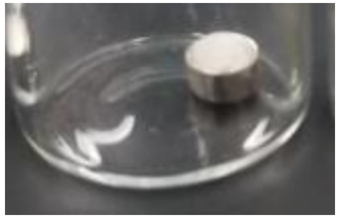

sanded

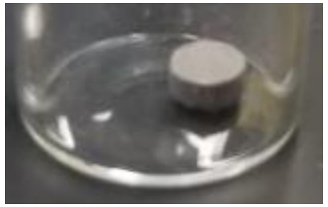

Oxidized 1 hour

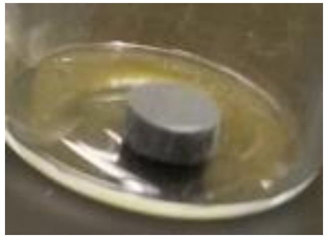

Oxidized 24 hours

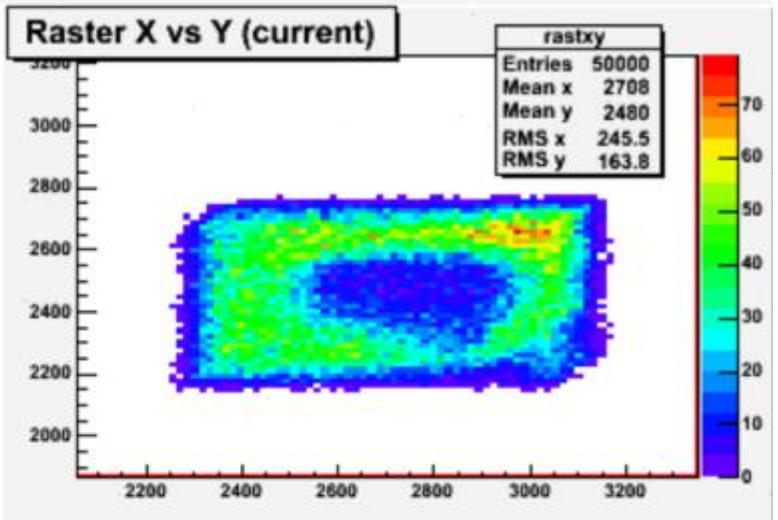

In PREX I, Pb target with thin diamond backing (4.5% bkgd) degraded fastest

Target with thick diamond (8% bkgd) ran well and did not melt at 70 uA

Target performance

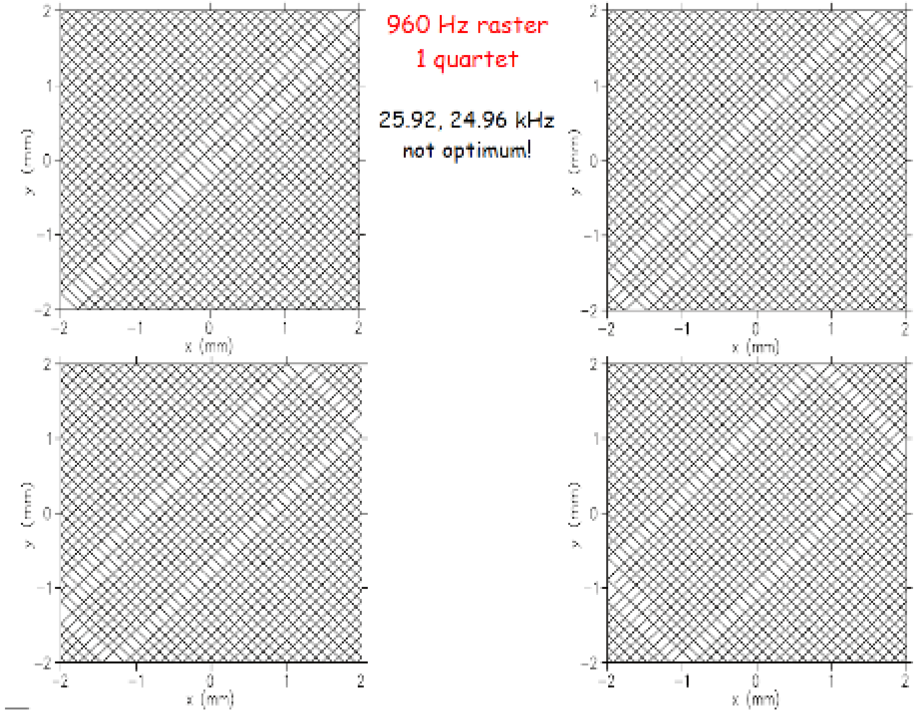

Solutions:

Sync the raster
Run with 10 targets

Acquire new ^{48}Ca
Don't expose it to air

Calcium target for CREX is currently in the scattering chamber

Vacuum is being monitored VERY closely

PREX II and CREX – happening now-ish

- The detector system performed really well – able to take ~2.5GHz on a 10 x 3.5 cm^2 piece of quartz in each arm
- Before beam corrections our combined detector widths were on the level of 200-300 ppm
- Regression allowed us to remove the added noise and gave us rock solid ~100 ppm widths throughout the run
- Asymmetry width provides measure of data quality

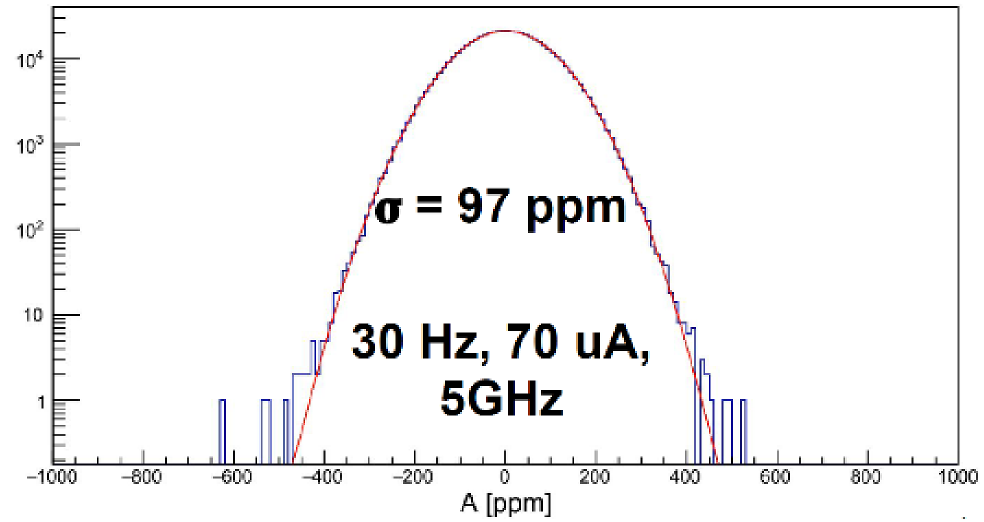

$$\sigma_A = \left(\frac{1}{flip\ rate} \times I\ (\mu A) \times R\ (Hz/\mu A) \times \#flips\ \times \#\ dets\right)^{-1/2}$$

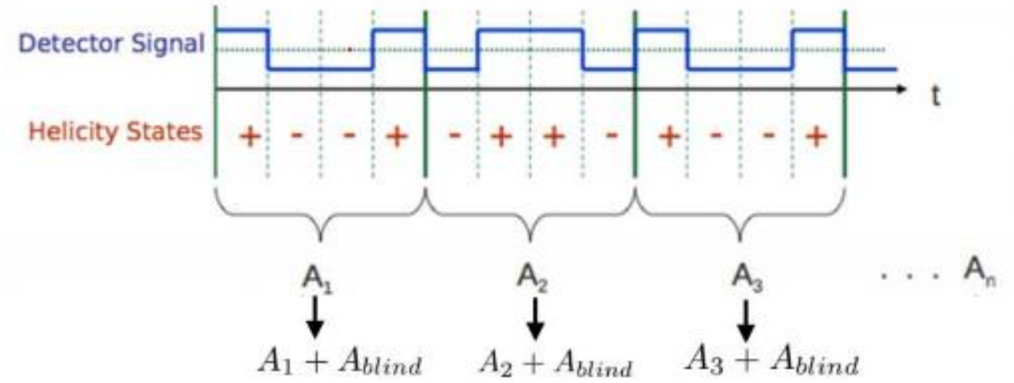

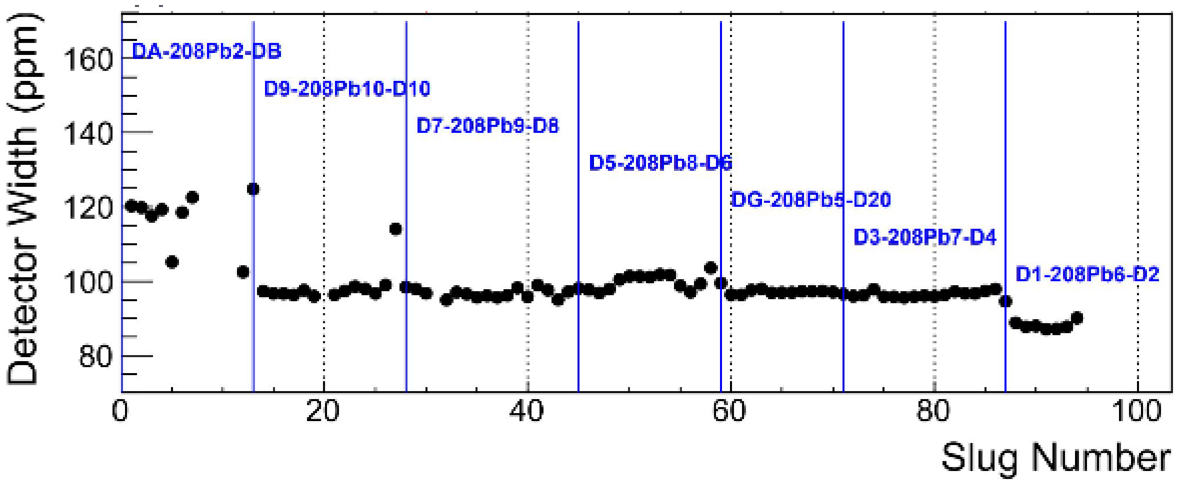

CREx run re-starts soon!

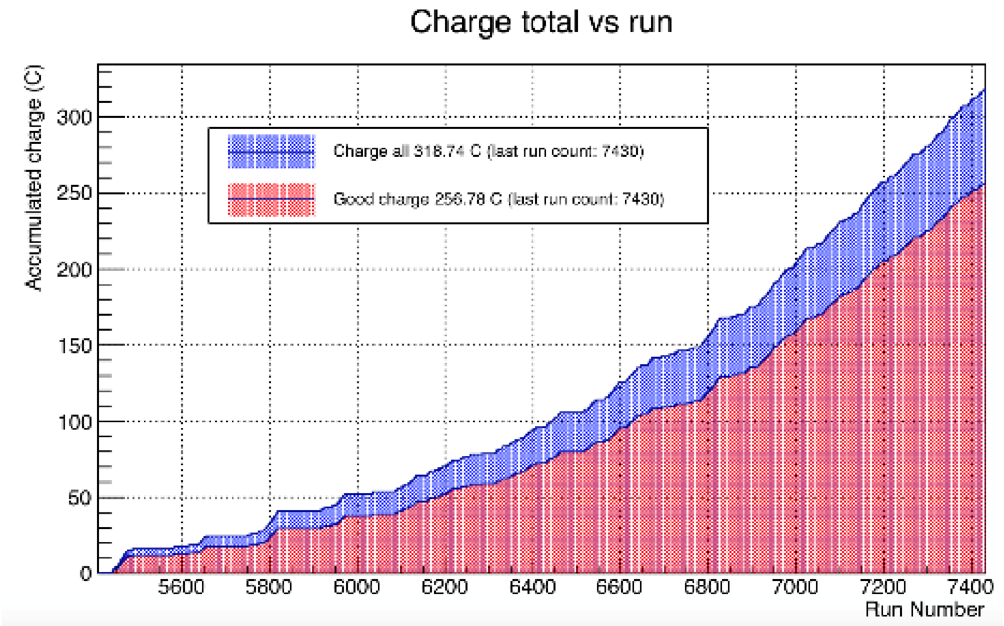

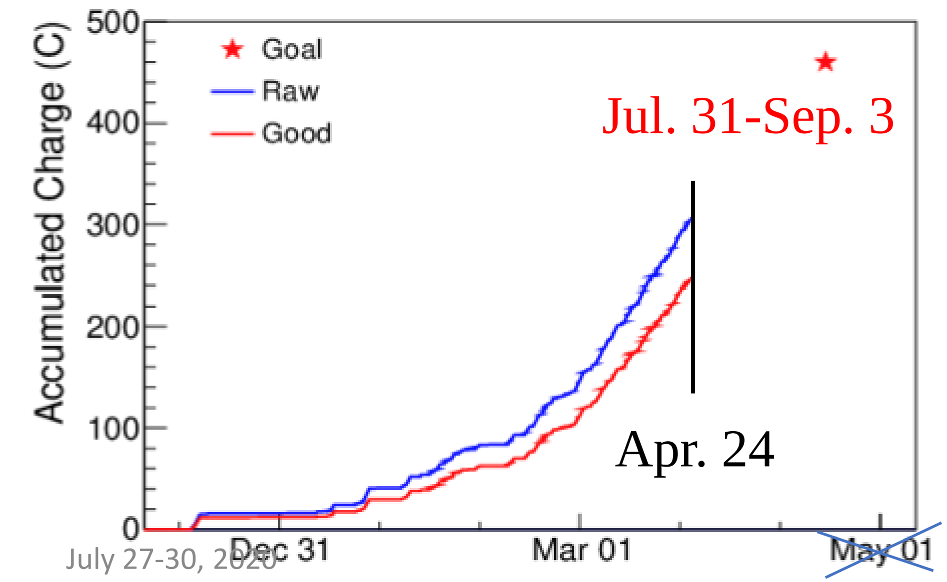

Goal: 453 C
Achieved: 54%

Need: 2C per shift to hit the goal, assuming we get all of the add'l time

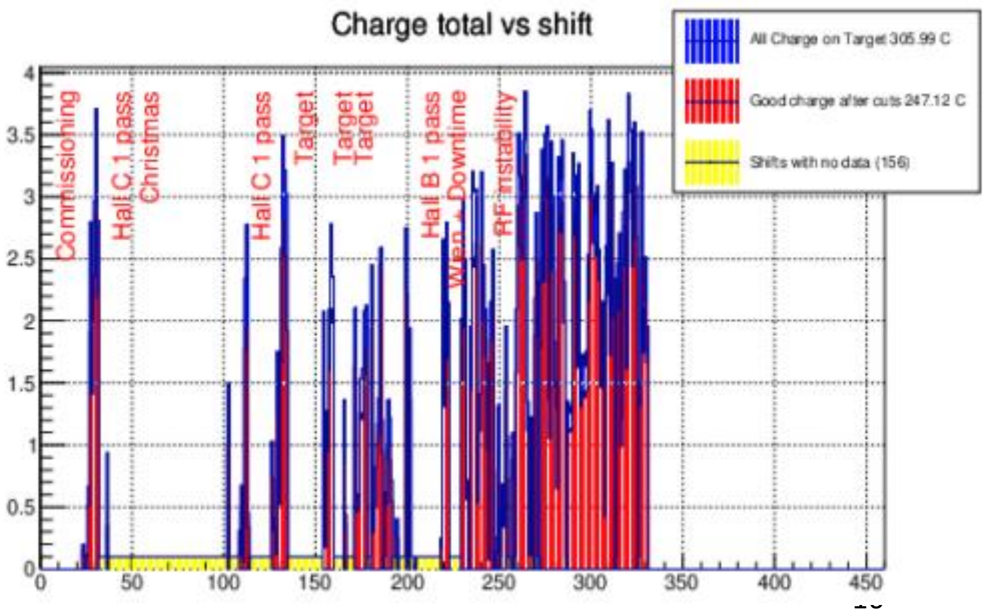

Regression Corrected Asymmetries

PREX-2 Data

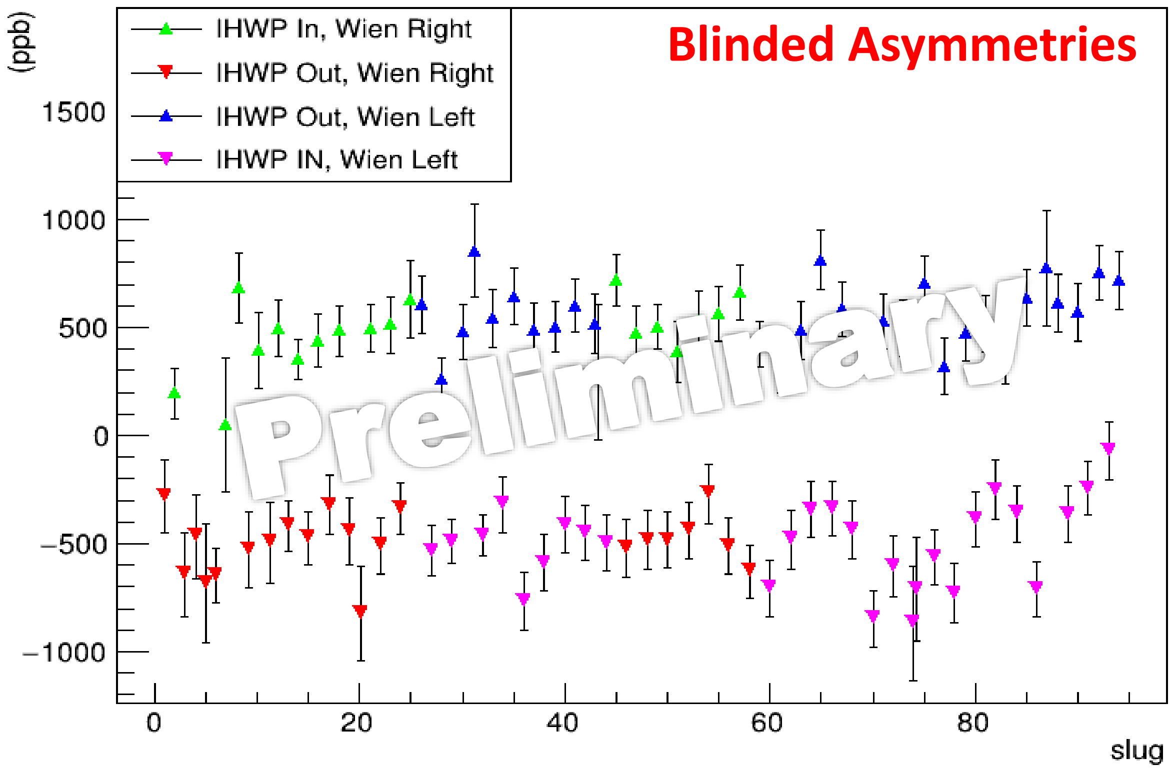

CREX Data

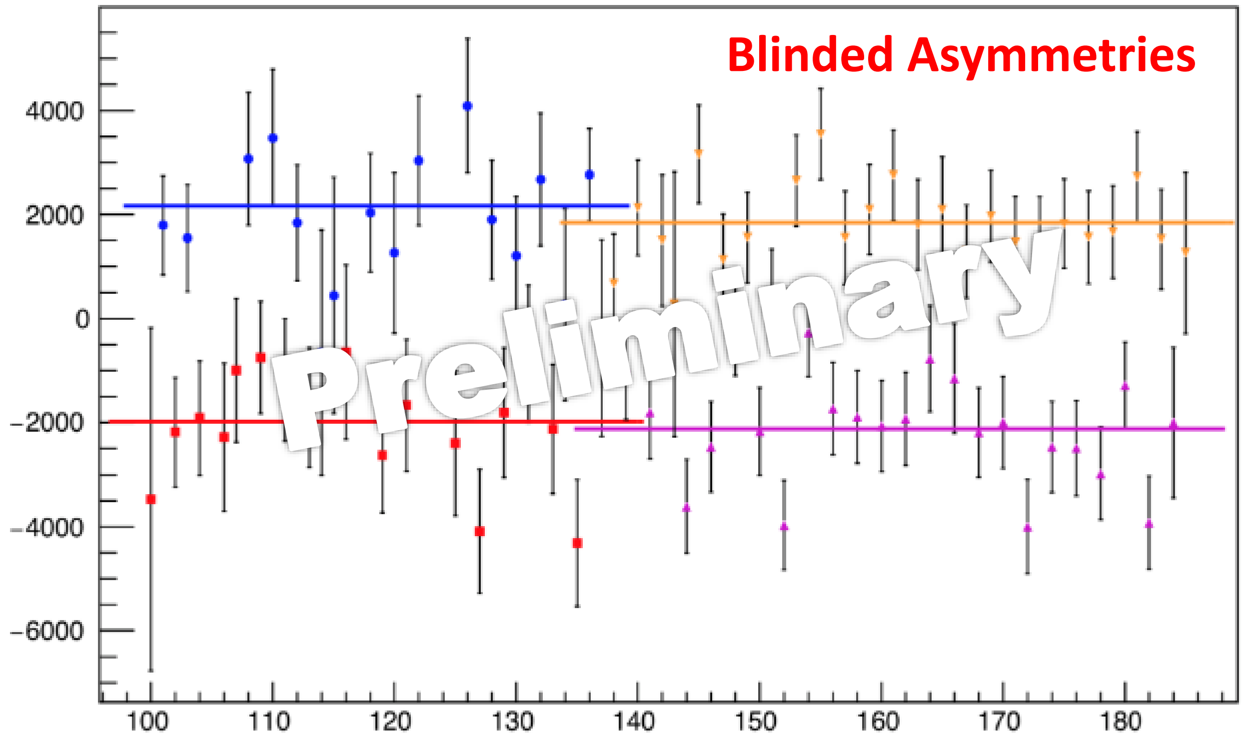

Analysis is ongoing, planned release at October DNP

Q^2 Acceptance – Optics measurements

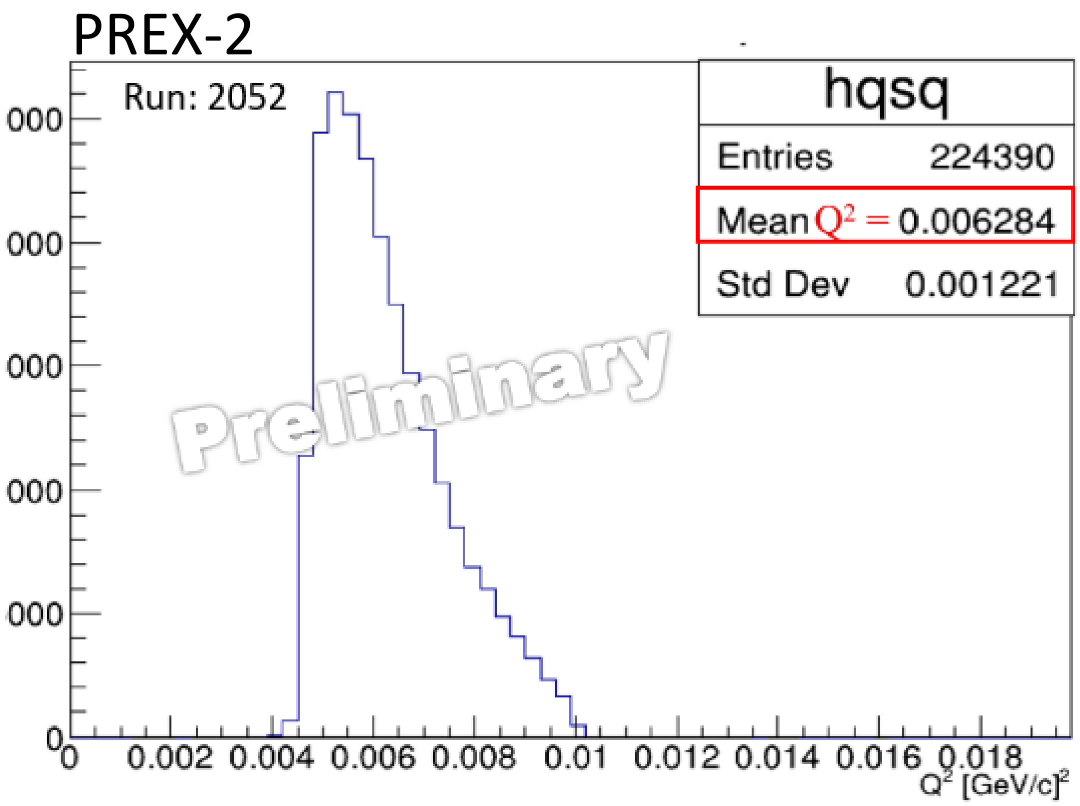

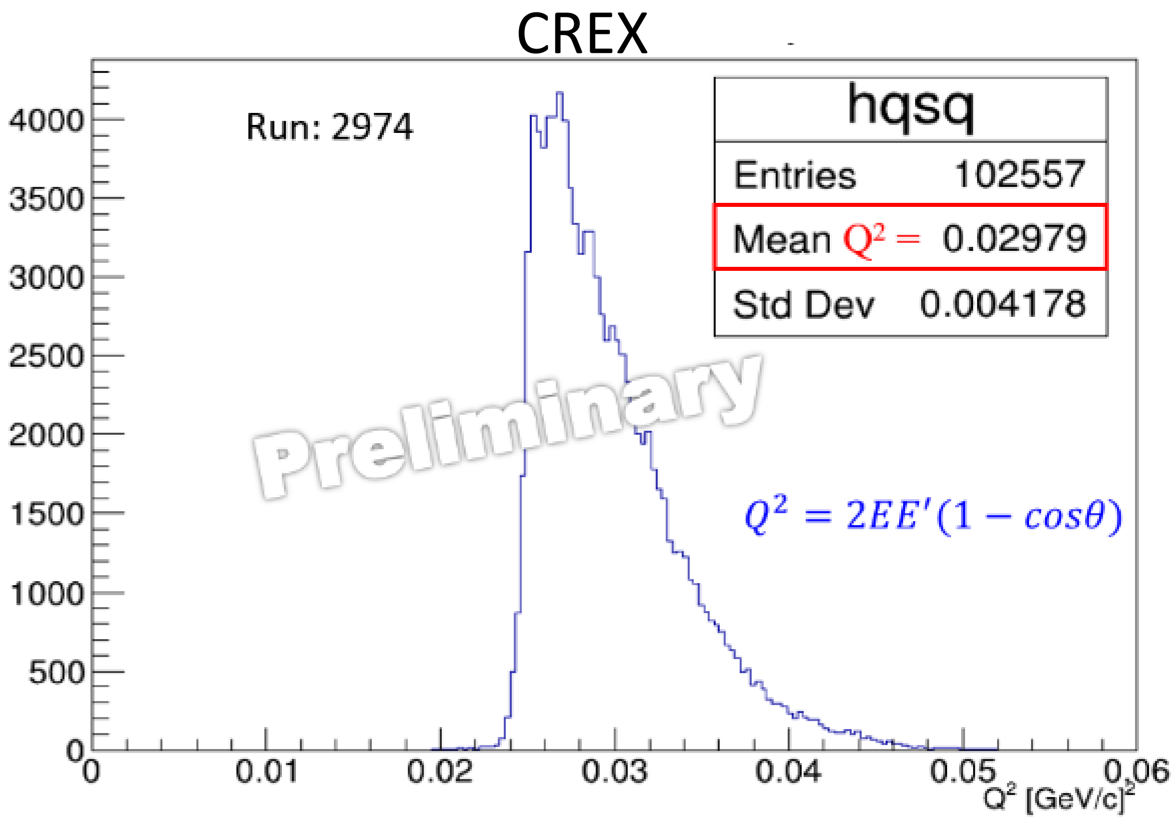

MREX

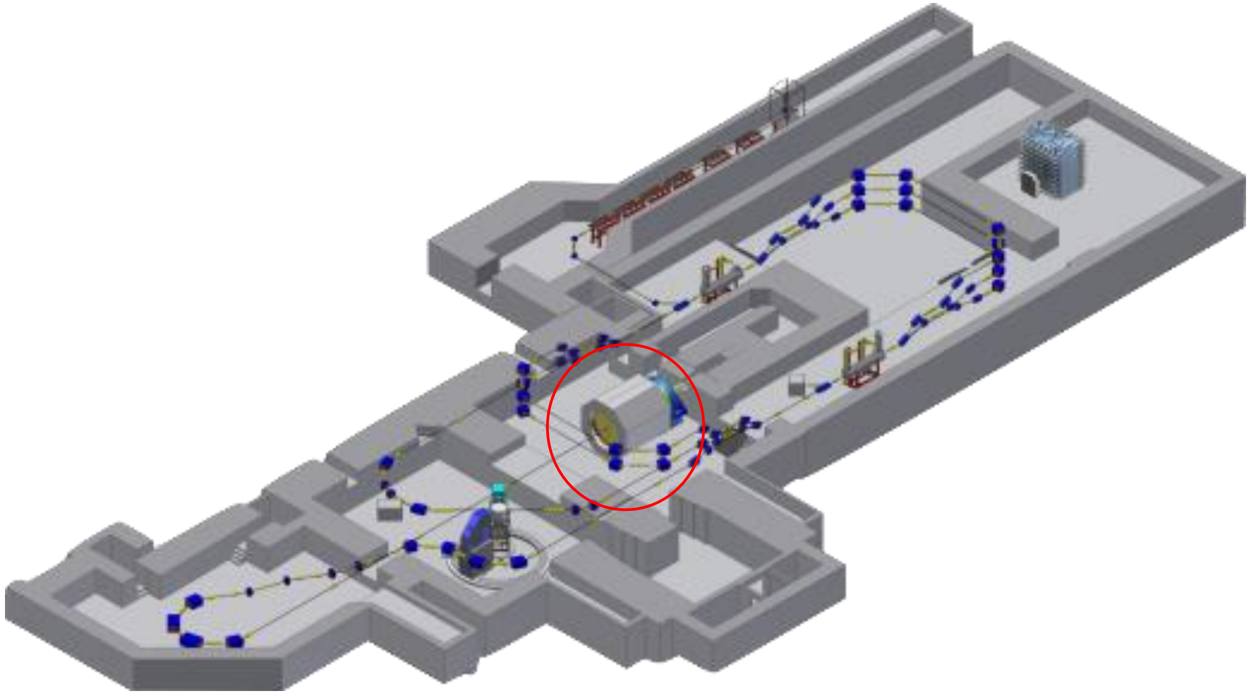

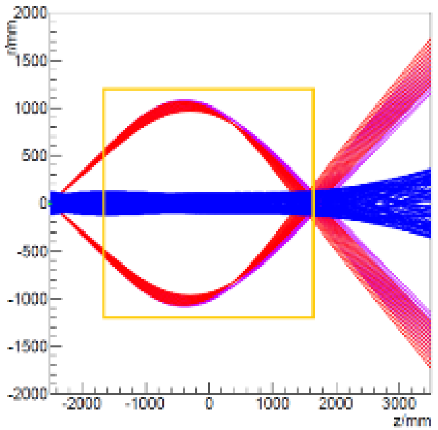

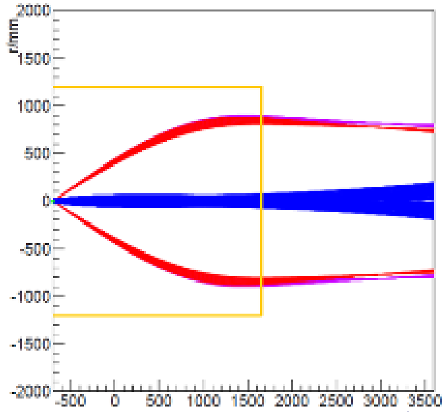

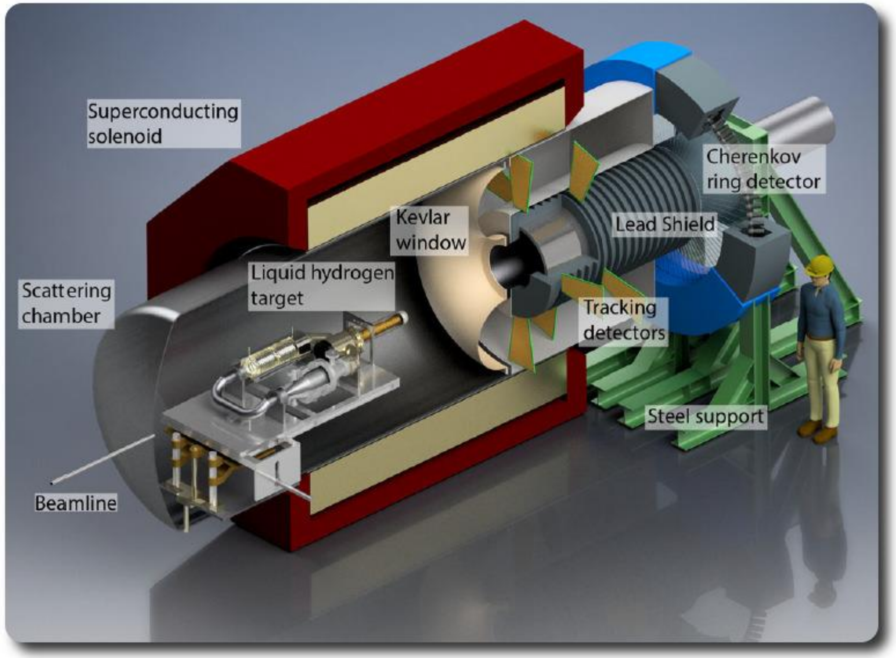

Choices to be made

- Detector configuration
- Beamtime limited to maximum 1500 hours
  - Pb or Ca?

Magnet/detector configurations

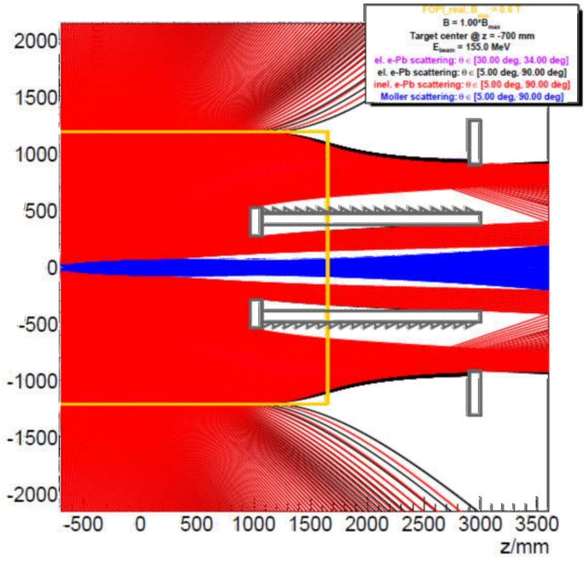

elastic e-, $30° < \theta < 34°$

inelastic e-, $30° < \theta < 34°$

Moller e-, $1° < \theta < 90°$

Need to be able to place the detector to choose the elastic peak

…with a minimum of backgrounds

and of course there are particles from $\theta < 30°$ and $\theta > 34°$

Extensive studies

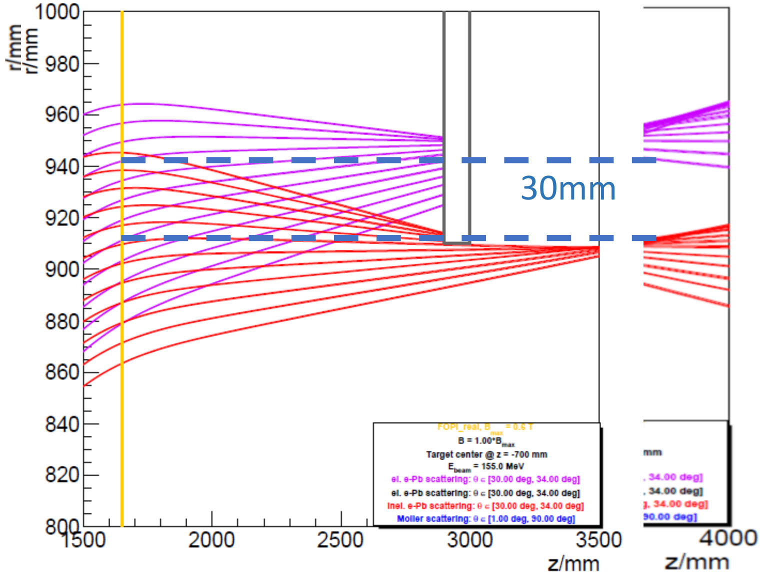

Michaela Thiel

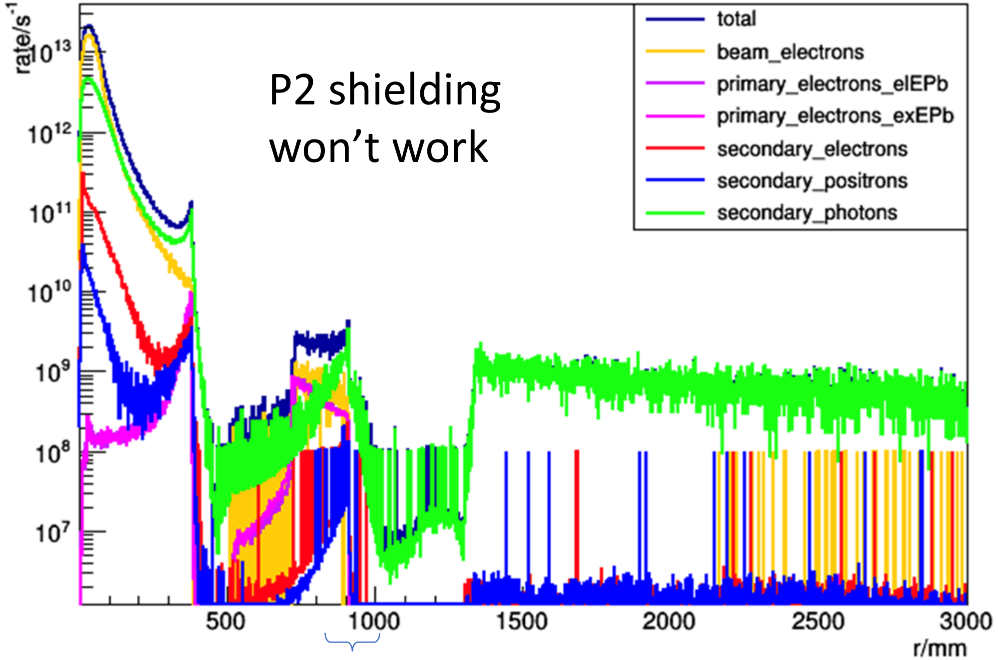

Range of plot to lower left

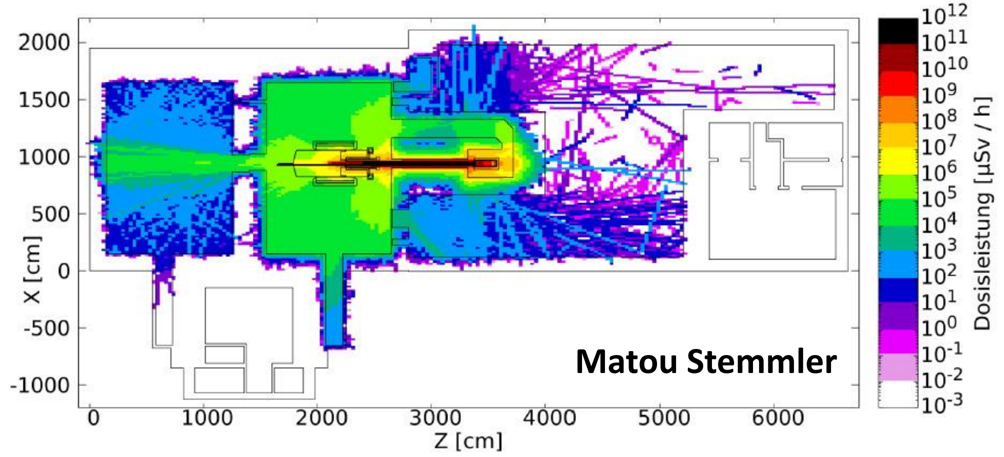

MREX

	MREX (Pb)	MREX (Ca)	PREX-2	CREX
Q (MeV)	86	143	79	170
Q (fm^{-1})	0.44	0.73	0.40	0.87
E_{beam}	155 MeV	155 MeV	950 MeV	2.2 GeV
$\delta A_{PV}/A_{PV}$	1.3%	1.3%	3.4%	5.7% (4.8%)
$\delta R_n/R_n$	0.52%	0.38%	1.3%	0.95% (0.8%)

$\Delta\theta=4°$: expected rate = 8.25 GHz, A_{PV} = 0.66 ppm, P = 85%, Q ≈ 86 MeV

1440h → $\delta R_n/R_n$ = 0.52% (^{208}Pb @ 155 MeV)

➢ **$\delta R_n/R_n$ = 0.5%**
→ L ± 20 MeV

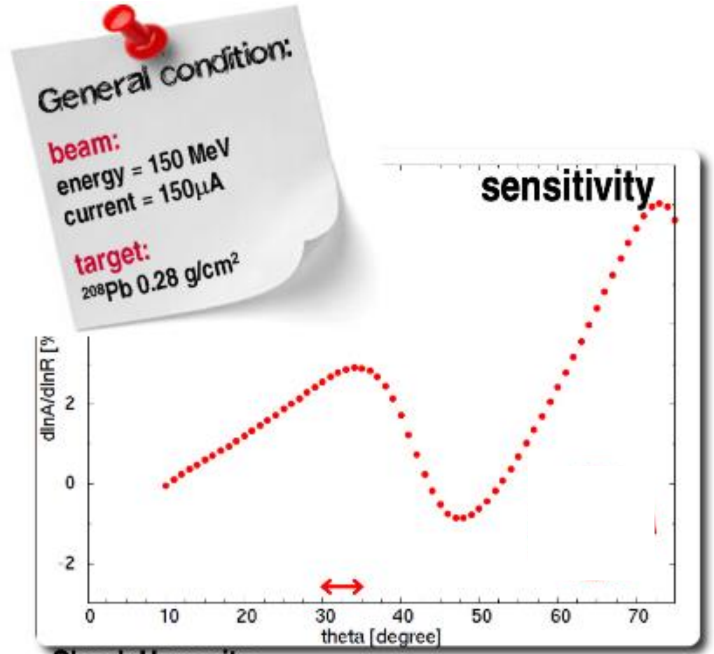

Chuck Horowitz

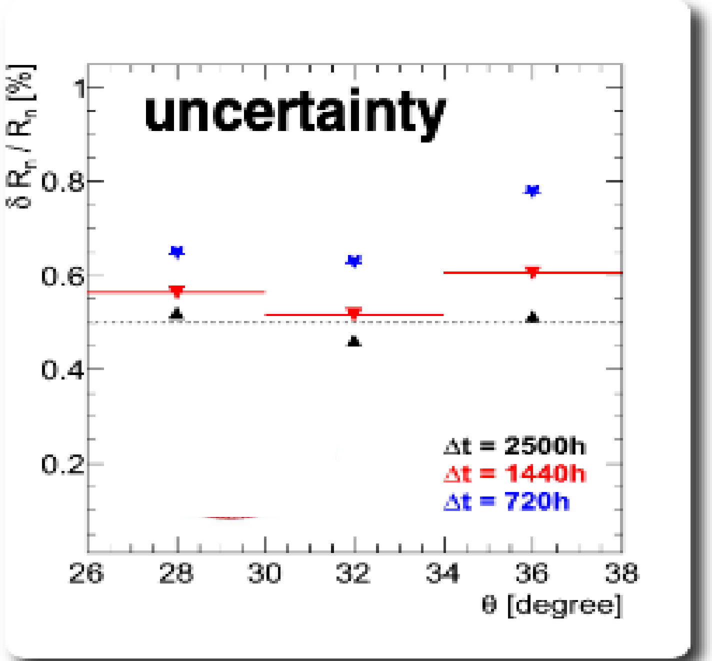

Michaela Thiel

Neutron Star Radii

Using models, one can relate the neutron star radius to the neutron skin of heavy nuclei

J. Lattimer and A. W. Steiner Astrophys. J 784 (2014)

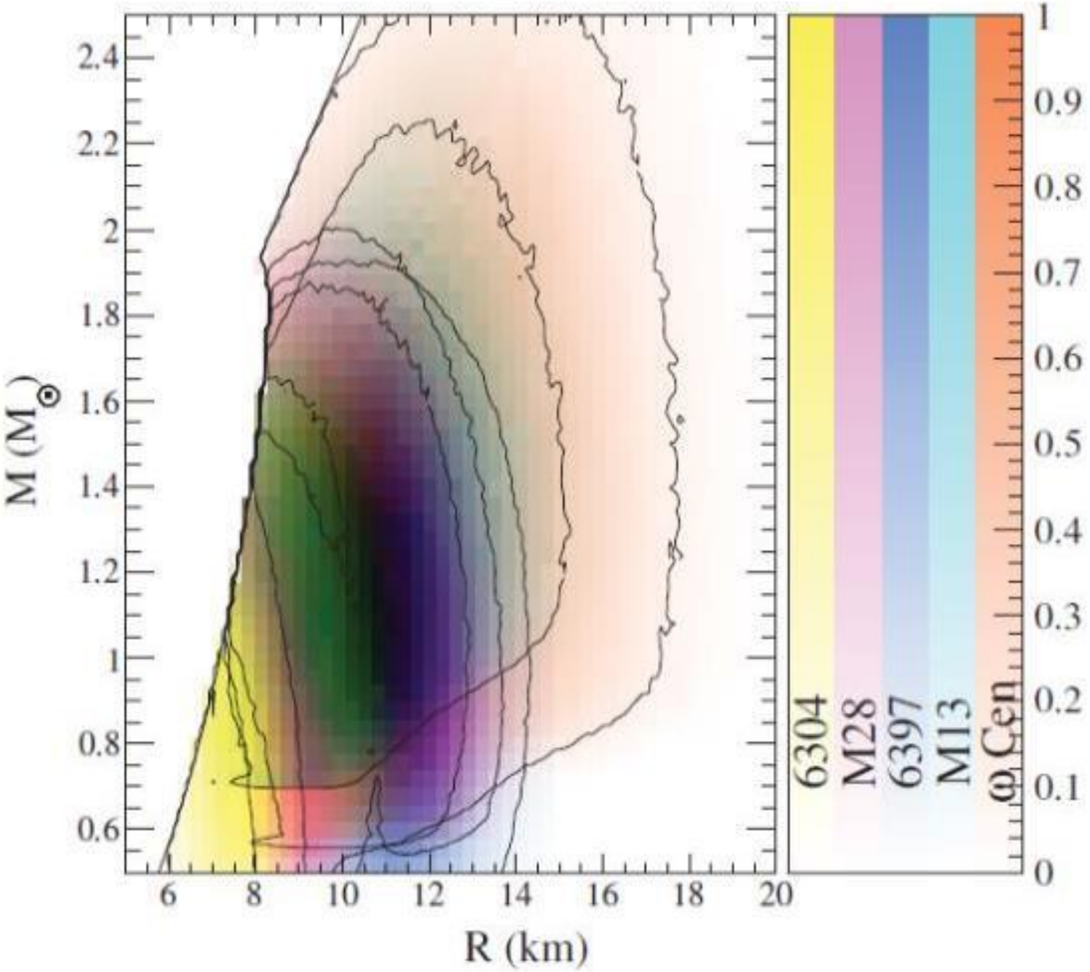

S. Gandolfi and A. W. Steiner J. Phys.: Conf. Ser. 665 (2016)

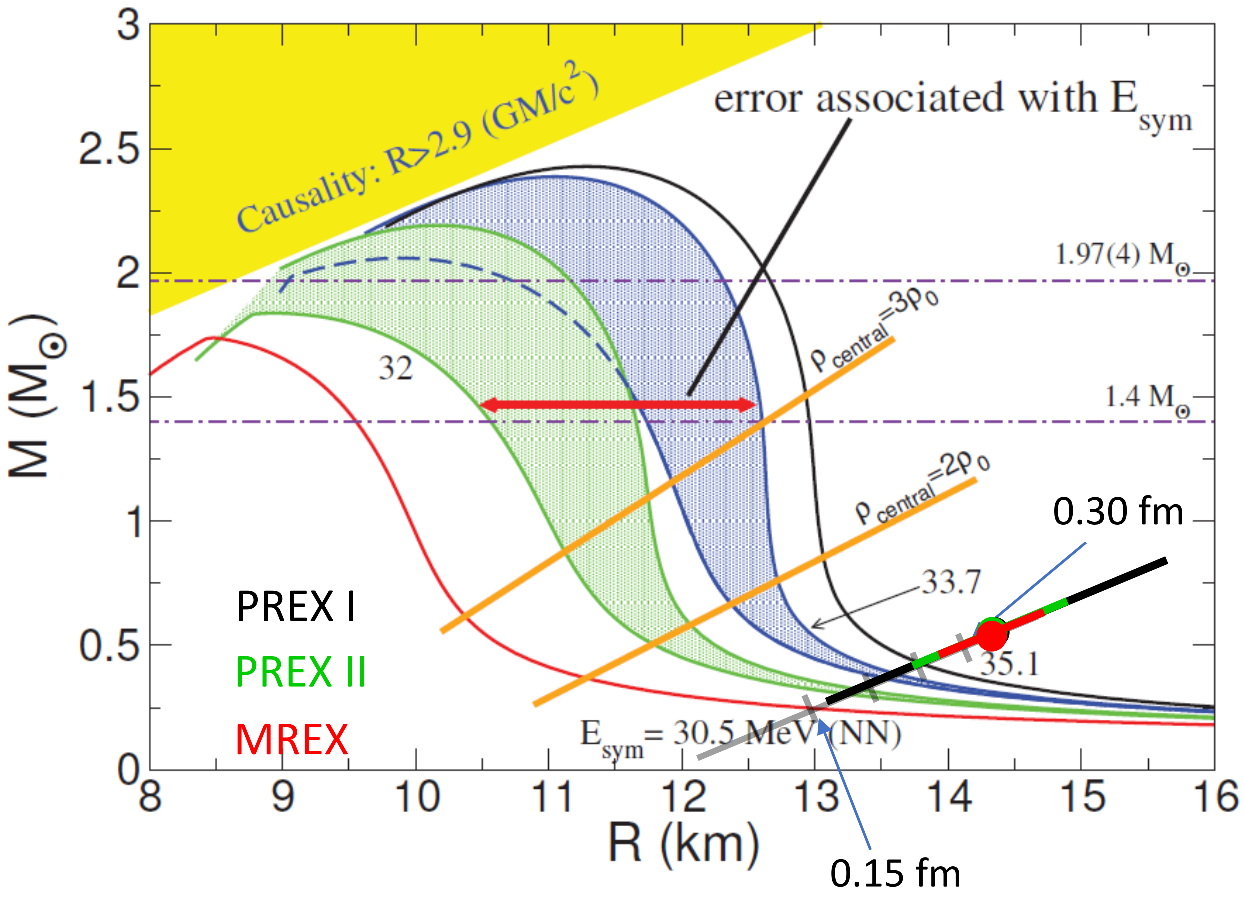

Including 3N forces changes the model predictions; CREX and PREX will help constrain the models

PREX

Kent Paschke *	UVa
Krishna Kumar	Stony Brook University
Robert Michaels	Jefferson Lab
Paul Souder	Syracuse University
Guido Urcioli	INFN Rome

* contact persons

CREX

Dustin McNulty *	Idaho State University
Robert Michaels	Jefferson Lab
Kent Paschke	UVa
Paul Souder	Syracuse Univeristy
Juliette Mammei	Manitoba University
Silviu Covrig	Jefferson Lab
Seamus Riordan	Argonne National Lab

J. Mammei, J. Birchall, M. Gericke, R. Mahurin, W.T.H. van Oers, S. Page
University of Manitoba

S. Riordan, P. Decowski, K. Kumar, T. Kutz, J. Wexler
University of Massachusetts, Amherst

K. Paschke, G.D. Cates, M. Dalton, D. Keller, X. Zheng
University of Virginia

P.A. Souder, R. Beminiwattha, R. Holmes
Syracuse University

R. Michaels, K. Allada, J. Benesch, A. Camsonne, J.P. Chen, D. Gaskell,
J. Gomez, O. Hansen, D.W. Higinbotham, C.E. Keppel, J. LeRose, B. Moffit
S. Nanda, P. Solvignon-Slifer, B. Wojtsekhowski, J. Zhang
Thomas Jefferson National Accelerator Facility

Konrad Aniol
California State University, Los Angeles

G.B. Franklin, B. Quinn
Carnegie Mellon Univerisity

D. Watts, L. Zana
The University of Edinburgh

P. Markowitz
Florida International University

P. Gueye
Hampton University

E. Cisbani, A. del Dotto, S. Frullani, F. Garibaldi
INFN Roma gruppo collegato Sanità
and Italian National Institute of Health, Rome, Italy

M. Capogni
INFN Roma gruppo collegato Sanità
and ENEA Casaccia, Rome, Italy

V. Bellini, A. Giusa, F. Mammoliti, G. Russo, M.L. Sperduto, C.M. Sute
INFN - Sezione di Catania

D. McNulty, P. Cole, T. Forest, M. Khandaker
Idaho State University

C.J. Horowitz
Indiana University

M. Mihovilovič, S. Širca
Jožef Stefan Institute and University of Ljubljana, Slovenia

A. Glamazdin
Kharkov Institute of Physics and Technology

T. Holmstrom
Longwood University

S. Kowalski, R. Silwal, V. Sulkosky
Massachusetts Institute of Technology

M. Shabestari
Mississippi State University

S.K. Phillips
University of New Hampshire

E. Korkmaz
University of Nortern British Columbia

P. King, J. Roche, B. Waidyawansa
Ohio University

C.E. Hyde
Old Dominion University

F. Meddi, G.M. Urciuoli
Sapienza University of Rome and INFN - Sezione di Roma

A. Blomberg, Z. E. Meziani, N. Sparveris
Temple University

M. Pitt
Virginia Polytechnic Institute and State University

D. Armstrong, J.C. Cornejo, W. Deconinck, J.F. Dowd, V. Gray, and J. Magee
College of William and Mary

D. Androic
University of Zagreb